RBRH
Revista Brasileira de Recursos Hídricos
Brazilian Journal of Water Resources
Versão On-line ISSN 2318-0331
RBRH, Porto Alegre, v. 29, e8, 2024
Scientific/Technical Article

https://doi.org/10.1590/2318-0331.292420230128

Characterization of woody material transport on the Madeira River at the Jirau Hydroelectric Power Plant: a study using a three-dimensional particle model

Caracterização do transporte de material lenhoso no rio Madeira na Usina Hidrelétrica Jirau: um estudo utilizando um modelo tridimensional de partículas

Isabela Rodrigues Caldatto[1], Ana Carolina Canossa Becker[2], Tobias Bleninger[1], Bruna Arcie Polli[2], Rubem Luiz Daru[2], Renato Penteado[2] & Claudiney Freitas[3]

[1]Universidade Federal do Paraná, Curitiba, PR, Brasil
[2]Instituto de Tecnologia para o Desenvolvimento, Curitiba, PR, Brasil
[3]Jirau Energia, Porto Velho, RO, Brasil
E-mails: ircaldatto@gmail.com (IRC), ana.becker.accb@gmail.com (ACCB), tobias.bleninger@gmail.com (TB), bruna.polli@lactec.com.br (BAP), daru@lactec.com.br (RLD), renato@lactec.com.br (RP), claudiney.freitas@jirauenergia.com.br (CF)

Received: October 25, 2023 – Revised: December 22, 2023 – Accepted: January 26, 2024

ABSTRACT

The Madeira River is characterized by large amount of woody material transported, especially during floods, which interferes with the operation of the Jirau Hydroelectric Power Plant. There are many logs and the log boom structures inserted to retain them do not always present the desired efficiency. This work involves the hydrodynamic simulation of the Madeira River and the three-dimensional simulation of these woody materials to analyze their trajectories along the river and to obtain knowledge of their transport and position according to the flow, different plant operations ways and the influence of log booms. The logs are simulated as particles by the PART module of Delft3d, using the Lagrangian particle tracking model. The hydrodynamic model was validated and it was possible to represent the main variations of three-dimensional velocities and water levels. The particle tracking simulation was consistent with the flow distribution and thus it was possible to identify the most attractive destination for the logs, according to power plant operations.

Keywords: Wood transport; Hydrodynamics; Particles; Lagrangian; Log boom; Reservoirs.

RESUMO

O rio Madeira é caracterizado pela grande quantidade de material lenhoso transportado, principalmente durante as cheias, e isso acaba influenciando as condições operativas tornando-se um grande desafio para a geração de energia na UHE Jirau. São muitos troncos e as barreiras flutuantes do log boom que tem a função de retê-los, nem sempre apresentam a eficiência desejada, em especial pelas inúmeras variáveis envolvidas e o regime de vazões. Este trabalho envolve a simulação hidrodinâmica do rio Madeira e a simulação tridimensional desse material lenhoso, para analisar seu comportamento ao longo do rio e ter conhecimento da sua posição conforme o escoamento, do seu destino e da influência das barreiras de log boom na hidrodinâmica e no transporte de partículas. Os troncos foram simulados como partículas pelo módulo PART do Delft3d, através do modelo Lagrangiano. O modelo hidrodinâmico foi validado e foi possível representar as principais variações de velocidades tridimensionais e níveis d'água. A simulação de partículas foi condizente com a distribuição de vazões e assim foi possível identificar, conforme a operação da usina, os destinos mais atrativos para os troncos.

Palavras-chave: Transporte de troncos; Hidrodinâmica; Partículas; Lagrangiano; Log boom; Reservatório.

INTRODUCTION

The Amazonian rivers are known for carrying large amounts of floating and submerged logs and debris, especially during flood periods. In the flooded areas occurs the dispersion of propagules that act as a physical structure for fauna shelter (Zuanon & Vilara, 2005).

The transport of woody material has been the subject of several studies in recent years. These studies have focused on ecological and geomorphological aspects (Ruiz-Villanueva et al., 2013). However, the numerical modeling of log transport in rivers is still a challenge and different strategies can be explored (Bladé et al., 2016).

Maintaining the sustainability of ecosystems presents a challenge when managing logs in river basins, as an excessive presence of these elements can lead to direct economic losses in hydroelectric plants, reservoirs, and navigation. On the other hand, a shortage of these logs can result in broader ecological issues for the entire river system, including increased sediment discharge, biodiversity loss, disrupted nutrient cycling, and even indirect consequences like flooding. While some countries have employed log removal practices to address these problems, the reintroduction of logs has been embraced in various restoration programs aimed at enhancing the hydrological, morphological, and ecological conditions of rivers (Ruiz-Villanueva et al., 2016).

Ruiz-Villanueva et al. (2014) developed a numerical model to simulate wood transport coupled with a 2D hydrodynamic model. The study consists of solving the shallow water equation in the hydrodynamic model including the k-ε turbulence model and representing logs by the Lagrangian model.

Bladé et al. (2016) discuss details of the numerical methods applied to the 2D model and highlight the main challenges of modeling woody material using the finite volume method. They simplify logs by not considering branches and roots and report on the difficulty of faithfully reproducing this material. They propose monitoring trunks to collect more accurate data.

Schalko (2018) discusses two-dimensional modeling of the accumulation of logs in river structures. Laboratory experiments were conducted to simulate the effect of log accumulation on bridge structures. Equations were developed to estimate the probability of this accumulation and the effect of backwater and erosion on bridge piers due to log transport. Continuing the research, Schalko et al. (2019) aimed to determine the parameters that govern the probability of accumulation and concluded that studying this phenomenon can help to identify critical sections and avoid problems such as flooding. With the increase in the number of hydropower dams, it has become essential to study about the correct management of woody materials to optimize the operation of the structures (Seo et al., 2010; Ruiz-Villanueva et al., 2016).

However, this specific topic is still scarce for large hydroelectric reservoirs. There are only a few cases that have been validated in the field, and the parameters for the modeling have not been fully clarified yet. Ruiz-Villanueva et al. (2014) and Schalko (2018) studies were applied to simplified situations of rectangular channels and to laboratory experiments, which cannot be applied to Jirau's size and complexity. Jirau Hydroelectric Power Plant (HPP) is located on the Madeira River which has a watershed approximately 974,000 km^2. The average flows in the Madeira River at the Porto Velho station (Hidroweb-ANA) vary between 22,000 m^3/s and 16,000 m^3/s. The increased flow beyond the decamillennial to the spillway flow for Jirau HPP is about 81,899 m^3/s.

In 2013, the Jirau Hydroelectric Power Plant began its operation and since then has been facing challenges in managing the large number of logs that are carried by the river, especially during the flood season. Different to many other rivers or log accumulation problems, the Federal Environmetal Agency requires that the logs are all passing the hydraulic structures and cannot be removed for environmental balance. Thus, structures have been installed to assist in the management of this woody material, such as a log spillway and log boom lines.

Log boom is a floating barrier composed of floats of plastic or metallic materials with front metal grids o flat plates and a system of anchors with chain moorings or cables connected to concrete boxes or anchors, forming floating lines on the river surface (Energia Sustentável do Brasil, 2019). This structure has the purpose of retaining and divert the logs so they do not reach the powerhouses, where they could either block the intake or even harm the turbines. It is estimated that during floods periods around 30,000 surface logs may reach the reservoir daily, part of them is supposed to be discharged downstream the dam by a log-spillway, during higher water levels, and discharged through the main spillways during high flow situations (Lactec, 2021). The log movement occurs every year and is always a critical situation. The most challenging moments can be identified during flood peaks, especially throughout the dam's history. According to the topographic features, the log channel region has a raised bed, and the flow of water suggests that most part of the woody material cannot reach the log-spillway and is retained at the log booms where their mechanized removal with navigation equipment is done on a daily base. Hereby, the logs are removed from the log boom, and transported to the spillway region, where they are discharged back to the river during spillway operation, or gates are temporally opened during lower flow periods to allow discharging the logs. The aim of this paper is to characterize the hydrodynamics of the reservoir analyzing different operational schemes of the power plant. As a first approach the woody material is represented as particles within a three-dimensional modeling suite and transported with a particle tracking model (Lagrangian model).

The influence of log boom structures on hydrodynamics and particle transport are also evaluated.

In this paper, two scenarios of plant operation were reproduced, a scenario with a closed spillway and another with an open spillway, both with and without log booms. It was analyzed how these scenarios affect the movement of particles, if the log booms interfere in the velocity fields, among other analyses.

MATERIAL AND METHODS

Study area description

The Madeira River is located in the northern region of Brazil through Rondônia and Amazonas states. Its source is located in the Andes Mountains, in Bolivia, where it receives the name Beni River. It is the 17th largest river on the world and has a watershed of 1,420,000 m^2 that drain areas in Brazil, Bolivia and Peru. It is 3,240 km long and flows into the Amazon River.

Carrying logs of forest plains to the riverbed is a characteristic of the river (Energia Sustentável do Brasil, 2019).

The Jirau HPP is located on the Madeira River, immediately downstream from Cachoeira do Inferno, at "Ilha do Padre" about 127 km upstream of the city of Porto Velho, capital of the state of Rondônia. The Madeira River, at the Jirau HPP, has a drainage area of 974,244 km^2 (Figure 1), corresponding to 69% of the total basin area (Energia Sustentável do Brasil, 2019). The annual mean discharge is approximately 40,000 m^3/s, according to ESBR (Energia Sustentável do Brasil, 2009).

The plant began operation in September 2013 and has 50 turbines, capable of generating 3,750 MW of power. The normal water level for operation is at elevation 90 m and the minimum water level at elevation 82.50 m above sea-level (Construserv Serviços Gerais Ltda, 2020). Jirau HPP is composed by the following structures:

- Right powerhouse – 28 turbines;
- Left powerhouse – 22 turbines;
- Spillway – 18 gates;
- Log-spillway: specific structure for discharging logs downstream the building. It works during rainy periods.

The Figure 2 shows the location of the Jirau HPP and the mentioned structures.

Hydrodynamic modeling

In order to achieve the objectives, the data provided by Jirau Energia was preliminarily analyzed and it was determined that the simulation should be able to represent hydrodynamic processes in a three-dimensional form. First, because the existing islands and an upstream groyne create 3-dimensional flow features (observed in ADCP measurements), second, because hydroacustic surveys observed that a portion of the logs are transported submerged in deeper regions. Among the models capable of simulating hydrodynamics with special features, such as log booms, Delft3D was chosen.

The Delft3D package has been developed by Deltares in the Netherlands and is composed of several modules with different simulation modules: hydrodynamics (FLOW), particle tracking (PART), sediment transport (SED), water quality (WAQ), and others.

The hydrodynamics module in the Delft3D solves the Navier-Stokes equations under the shallow water approximation, a system consisting of the continuity (mass balance) and momentum equations for free surface flows. It disregards accelerations in the vertical direction because it assumes hydrostatic pressure distribution.

The model uses horizontal orthogonal curvilinear coordinates to smooth out errors in modeling the curvature of the riverbed, and these can be Cartesian coordinates (ξ,η) or spherical coordinates (λ,ϕ).

Vertically, the model can use the sigma (σ grid) or Cartesian (z grid) coordinate system. This paper uses the sigma coordinate system, where the number of layers is constant and only their thickness varies. The grid is bounded by the bottom topography and the free surface.

Turbulence is solved using Reynolds decomposition and has four closure models: constant coefficient, algebraic method, $\varkappa$-L model, and $\varkappa$-ε model. Here, the $\varkappa$-ε model is used, where $\varkappa$ is the turbulent kinetic energy and ε is the dissipation rate of this energy (Deltares, 2023a).

Model setup

The computational mesh was defined from the reservoir boundary (Figure 3) and is a three-dimensional grid of five layers, following the vertical sigma coordinate system (σ-model), shown in the Figure 4.

In Delft3D, two coordinate systems are available for the vertical resolution. The terrain following sigma coordinate system and a vertical fixed grid system. First has advantages in the shallow regions, as it has high resolution there. Latter has advantages in stratified systems. For a fluvial hydrodynamic flow situation, it is recommended to have higher resolutions close to the bed, to represent better the logarithmic velocity profile.

Figure 1. Madeira River watershed from the Jirau Hydroelectric Power Plant.

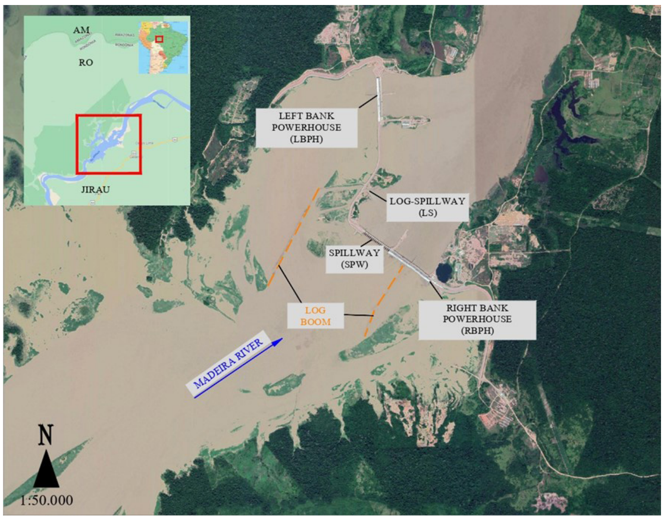

Figure 2. Jirau Hydroelectric Power Plant structures.

For wind induced flows, it is the opposite. However, the option was chosen to make a uniform distribution vertically and still have a 3D model, as an alternative approach to the other studies.

The dam structures were represented by Delft3D's "Thin Dams" tool, which prevents water from flowing between two cells.

To represent the spillway and discharge in the powerhouses, the "discharges in-out" tool was used, which takes a series of steady or time-varying flows from one cell and places them in another. This tool allows uniform flow distribution (along the powerhouse length) and different flow rates for each unit. The program also allows "dry cells" to be placed to represent islands or paths that do not pass water. To illustrate the tools used, Figure 5 zooms in on the right bank powerhouse (RBPH) and spillway (SPW). In yellow are the "thin dams" bounding the dam structures, in green are the dry cells, and in purple are the spillway and RBPH structures containing the flow series information.

The bathymetry was obtained through campaigns carried out by the Lactec team. In 2021, a topographic survey was carried out using laser equipment (LIDAR), which flew over the reservoir and riparian areas. This survey made it possible to obtain a Digital Terrain Model (DTM) of the regions at the bottom of the reservoir that were exposed due to the dry period. In the same year, Lactec carried out bathymetry of the reservoir using single-beam and multibeam equipment, resulting in a significant improvement in the physical boundary conditions, as well as providing the necessary updates for modeling.

Therefore, the bathymetric coordinates at the grid nodes were obtained by interpolating the existing bathymetric data using the Quickin tool in Delft3D (Figure 6). Elevations equal to zero correspond to the orthometric elevation of 90 m, i.e., the normal water level.

Two open boundary conditions were defined for the reservoir domain, upstream and downstream (Figure 6). The upstream boundary condition was a constant discharge time-series, applied uniformly over the transect. The downstream boundary condition was a water level, which was taken from the rating curve and corresponding to the upstream discharge.

The model has the same domain and same settings for all scenarios that were simulated. There are 24 hours of simulation with a time step of 0.05 minutes. Physical processes such as wind, temperature components or sediments were not considered here. This was justified, because the reservoir is a run-of-a-river reservoir, with large (order or meter per seconds) flowrates, thus negligible wind effects. Observations also showed no density stratification at no time. Uniform values were entered in the initial water level condition, equal to 0.34 m, which means 90.34 m level in the reservoir, and zero velocities as starting point. The physical parameters are described in Table 1.

Table 1. Physical Parameters.

Parameter	Value	Unit
Water density	1,000	kg/m³
Roughness (Manning)	0.035	-
Horizontal Viscosity	1	m²/s
Vertical Viscosity	3D turbulence model: k-ε	-

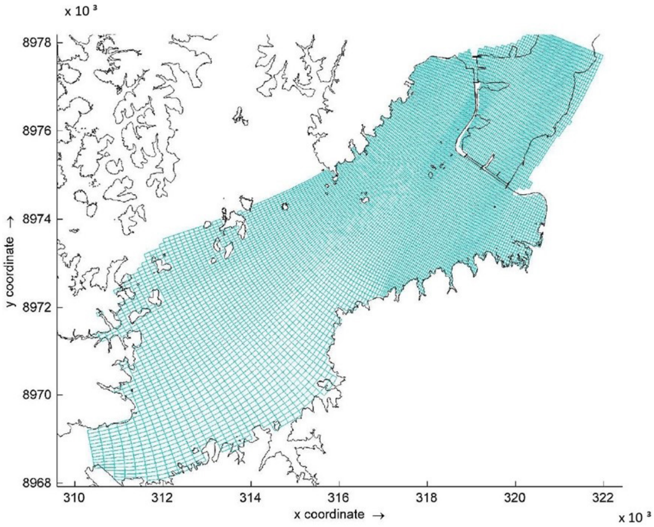

Figure 3. Computational Mesh – Planar view.

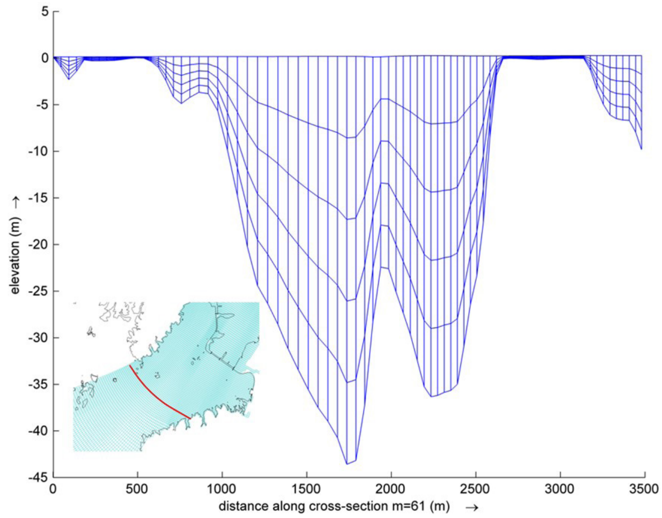

Figure 4. Vertical grid using sigma coordinate system in a reservoir section.

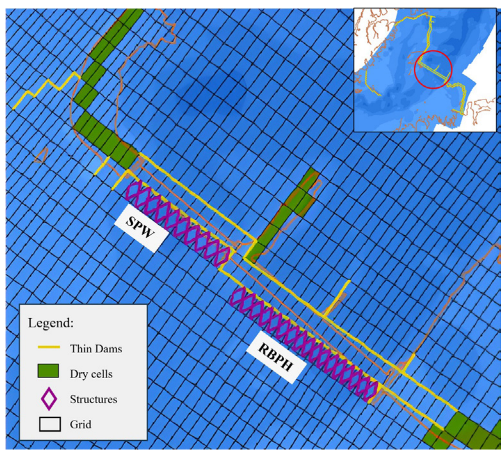

Figure 5. Representation of the dam structures implemented in the Delft3D model. Zoomed image in SPW and RBPH. Scale: 1:10.000.

The log booms were also represented in the model as surface structures added in the first layer of the model. They were implemented in the Delft3D using the “3D gates” tool, which is a vertical plate along one of the grid directions that can cover the flow in a predetermined number of layers vertically from the surface, as shown in the illustrative scheme in Figure 7. The Figure 8 shows the position of the log booms.

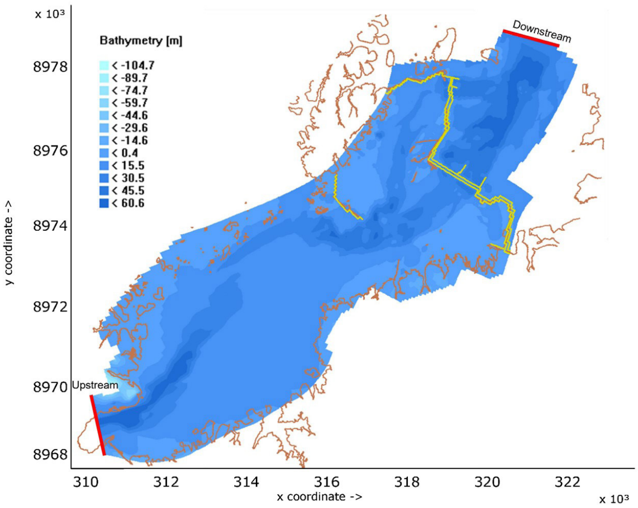

Figure 6. Interpolated bathymetry data and boundary conditions.

Calibration

The model was calibrated using measured data from an Acoustic Doppler Current Profiler (ADCP), an acoustic device that uses the Doppler effect by emitting sound pulses and detecting the echoes from suspended particles, and reservoir level data. The result is represented in pixels, each of which, in a cross section, has the value of the intensity and direction of the water velocity. By integrating in the section, is possible to compute the flowrate that passes through a section.

Four scenarios were chosen: high flow, intermediate flow, low flow and lower flow (Table 2). The Delft3D model was used to simulate the situation that occurred in these four cases, using the plant’s operational information.

The measurements were taken from the section shown in Figure 8 bottleneck section called “Bananal”.

Table 2. Scenarios for comparison with ADCP data.

Scenario	Date	Discharge (m^3/s)
High Flow	25th Feb 2019	41,590
Intermediate Flow	11th Feb 2017	20,072
Low Flow	16th Aug 2018	6,808
Lower Flow	09th Aug 2016	3,599

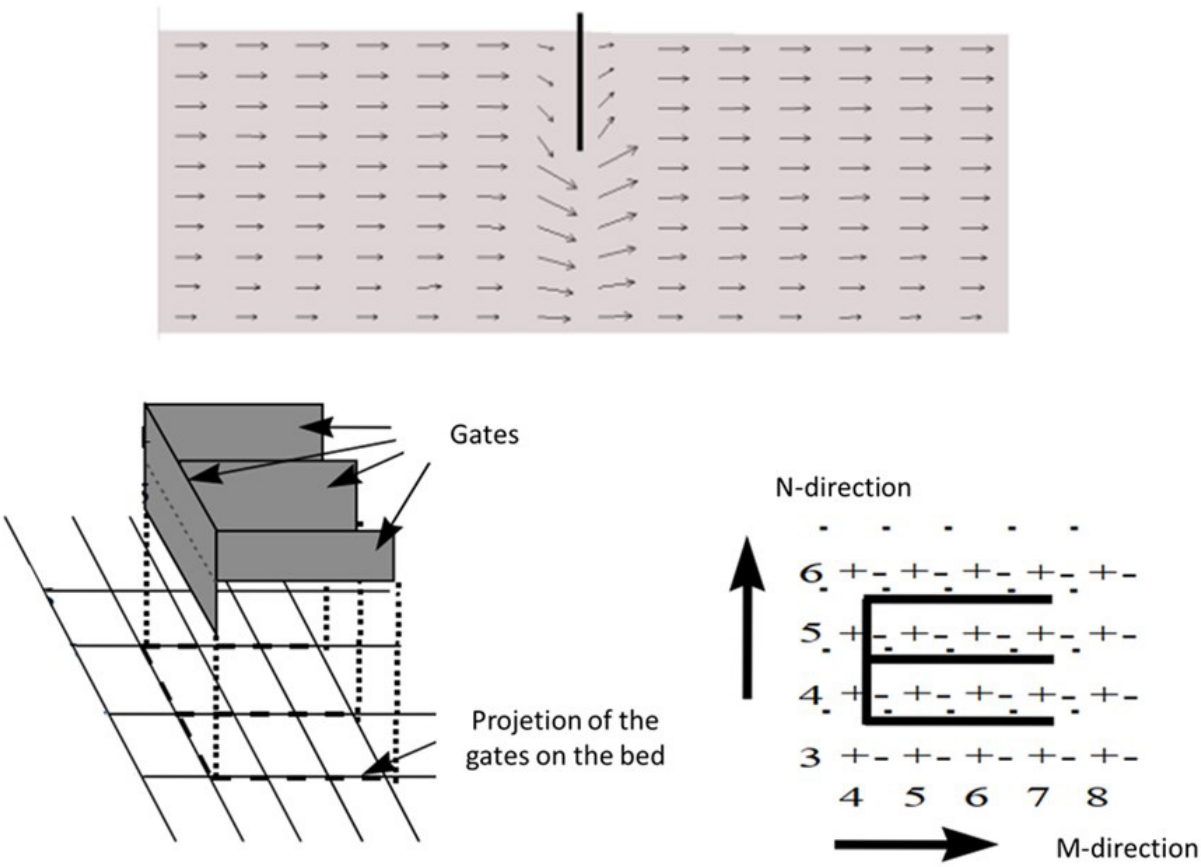

Figure 7. Illustrative example of the “3D gate” structure in a cross section (Deltares, 2023a).

Operational scenarios

To quantify the operational effects on the flow pattern, as well as the influence of log booms, two hypothetical scenarios with different operational modes and different flow conditions were defined (Table 3). These discharges and scenarios result from both actual operational tests and hypothetical optimization processes aimed at determining whether specific operational measures can enhance log transport through the structures. Scenario 1 considers full operation of powerhouses without spillover. Scenario 2 considers normal operation with full opening of Clapet gates at the spillway ends. A fully open Clapet gate corresponds to a partial opening of a standard gate at its top, thus allowing floating material to pass through.

The abbreviations RBPH, LBPH, SPW, and LS correspond to right bank powerhouse, left bank powerhouse, spillway, and log-spillway, respectively.

Both scenarios were simulated for situations without retaining structures and using a surface log boom.

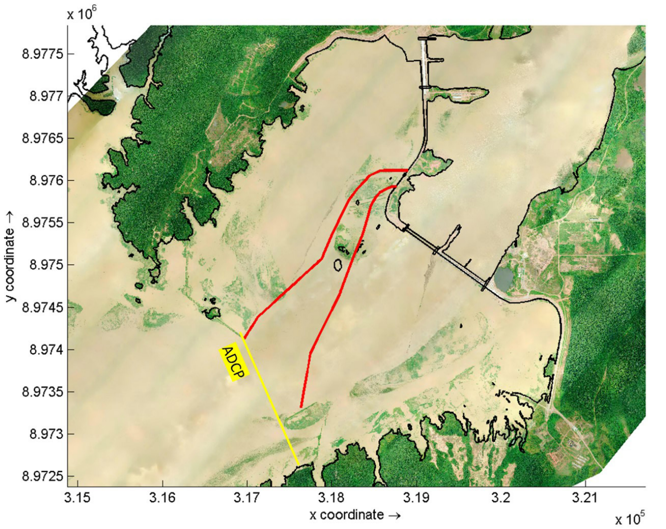

Figure 8. Schematic representation of log booms positions in red and ADCP section in yellow.

Particle tracking model

For woody material transport simulation, the simplifying assumption was used that the velocity and movement of logs follow the velocity of the flow, i.e., a particle model coupled to the hydrodynamic model. This assumption has already been applied in other log transport modeling methods with good approximation (Ruiz-Villanueva et al., 2014).

For this particle tracking simulation, the logs were represented as particles with no mass and no volume that follow the flow (Lagrangian modeling). The Delft3D-PART model coupled with Delft3D-Flow was used for this simulation.

Particle tracking models are based on the principle that the motion of substances can be described by a large number of particles moving randomly through horizontal and vertical dispersion. This principle is also known as "random walk". The particles are also subject to advection due to shear (bottom) and wind (surface) stresses (Deltares, 2023b).

It is possible to release continuous or instantaneous particles. In the current case, particles were released instantaneously upstream of the bottleneck section, at 8 points along the section (Figure 9). After verifying that the number of particles does not change the statistics, it was decided to release 20 particles at each point.

The most important parameters that can affect particle tracking are the vertical and horizontal dispersion (Deltares, 2023b). The horizontal dispersion was calculated by the model) shown in Deltares (2023b, p. 103).

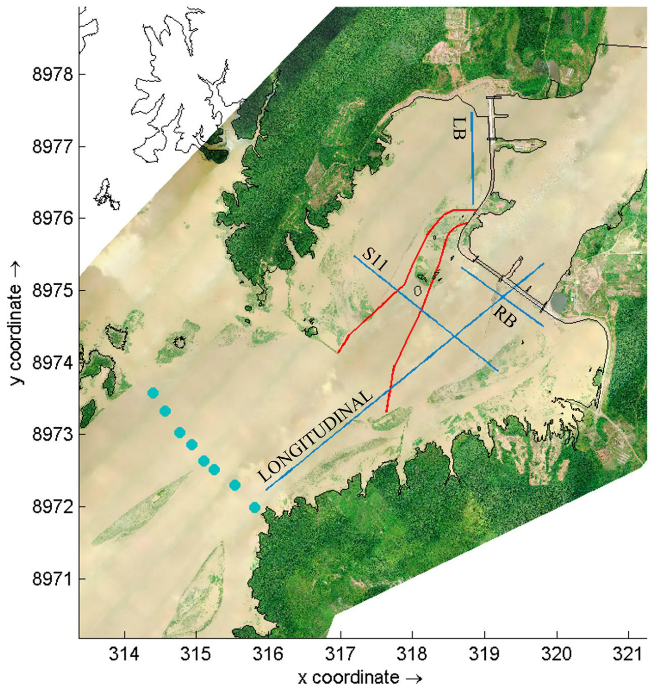

Figure 9. Instantaneous particle release points represented by blue dots; Sections for checking velocities in cross sections on the right bank (RB), left bank (LB), section across log booms (S11), and longitudinal section along the reservoir.

Table 3. Operational Scenarios.

Scenario	Description	Level (m)	Total Discharge (m^3/s)	Discharge RBPW (m^3/s)	Discharge LBPH (m^3/s)	Discharge SPW (m^3/s)	Discharge LS (m^3/s)
1	Full operation of powerhouses without spillover	90	27,800	15,400	12,100	0	300
2	Normal operation with full opening of Clapet gates at the spillway gates 2,3,4,16,17,18	90	29,800	15,400	12,100	2,000	300

Field measurements (Lactec, 2023) showed that approximately 90% of the logs are transported at the surface. This number can vary in curves or close to the intakes, due to secondary currents or alike. This was the reason to release the logs at the surface in a cross-section after a long straight flow. Tests were performed for a buoyancy velocity (negative); however, the model only works with a sedimentation velocity (positive).

Therefore, a zero buoyancy was set due to limitations of Delft3D in that regard and have the best validation when compared to the data measured in the field.

The movement of the particles is influenced by the hydrodynamic data from Delft3D-Flow. The particles positions follow the three-dimensional velocities at each time step. In addition, they are dispersed in proportion to the simulated turbulence. The trajectories are displayed in 3D and the particles can pass the vertical layers by their vertical movement.

RESULTS AND DISCUSSIONS

Calibration

To calibrate and verify the model, and to understand the hydrodynamic flow in this region, a comparison of the ADCP measurements with the Delft3D simulation results was performed. From Figure 10 to Figure 13 these comparisons are shown for the highest flow scenario (41,590m^3/s). The results of the other three scenarios are presented in Appendix A.

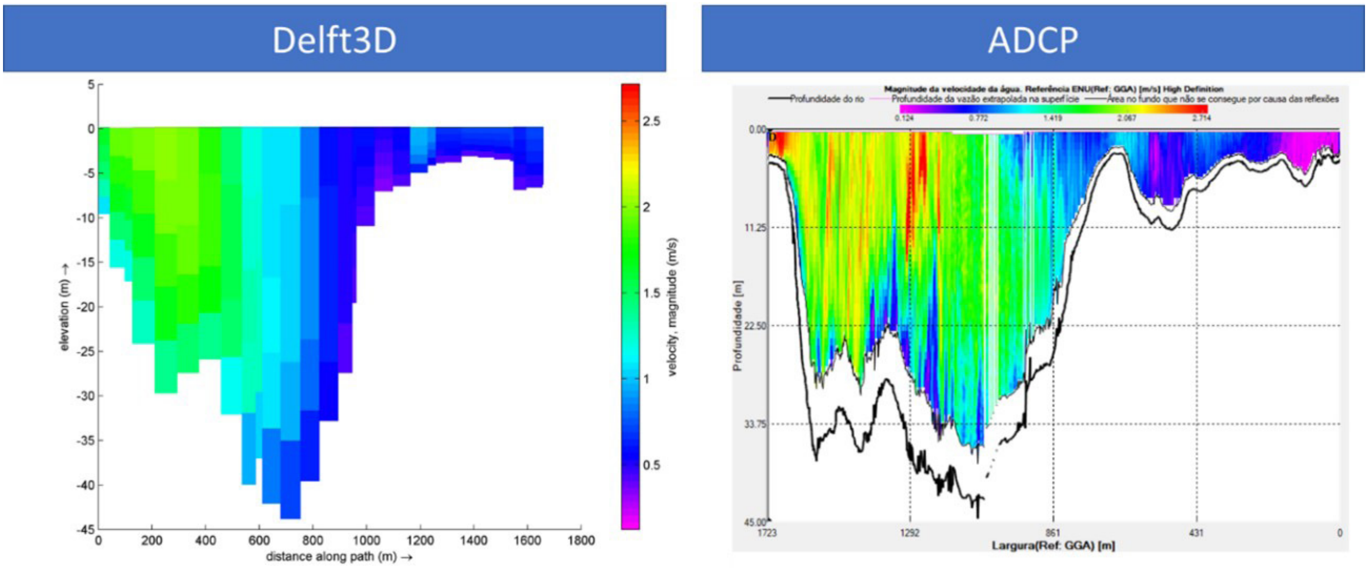

Figure 10. Transect illustrating magnitude of horizontal velocities - High flow - 25th Feb 2019.

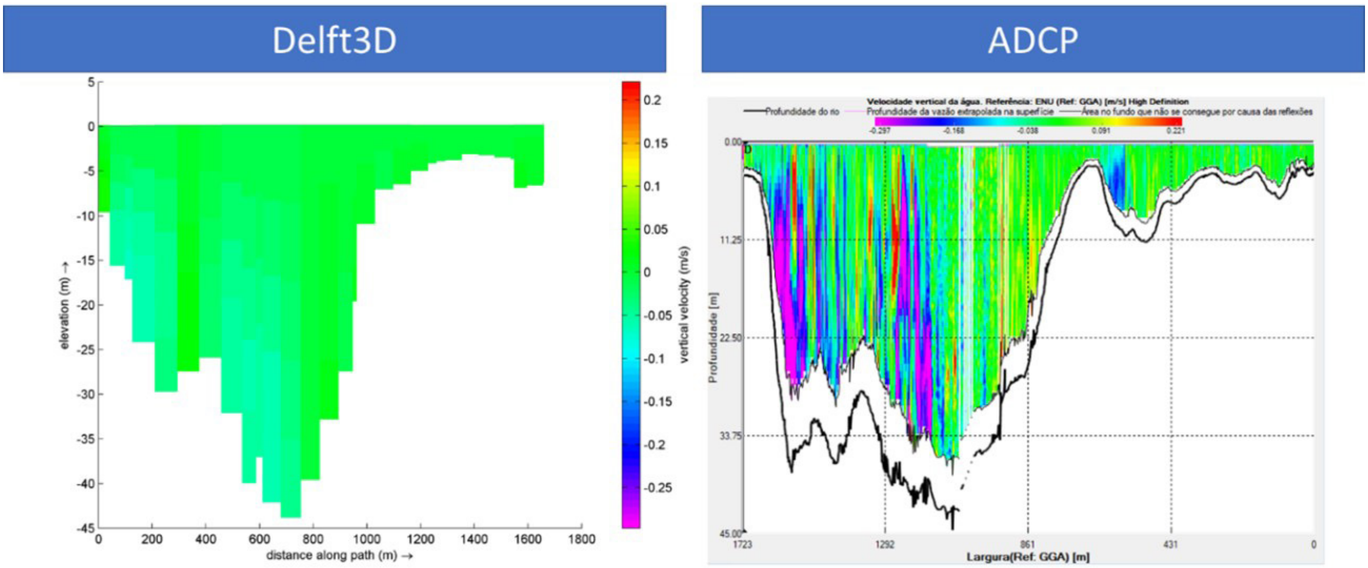

Figure 11. Transect illustrating magnitude of vertical velocities - High flow - 25th Feb 2019.

It was observed that the Delft3D model qualitatively shows velocity fields similar to the ADCP measured results in the higher flow scenarios (flows of 20,000m^3/s and 40,000m^3/s approximately) in both magnitude and direction of velocities. However, at low flows, particularly at the 6,808 m^3/s flow scenario, the Delft3D did not represent the ADCP results in a similar manner. At this flow rate, the Delft3D showed higher velocities on the left side of the section and the ADCP on the right side of the section (Figure 14). In addition, the vector figure (Figure 12) are not having the same scale, unfortunately, as the raw data wasn't available for quantitative comparison.

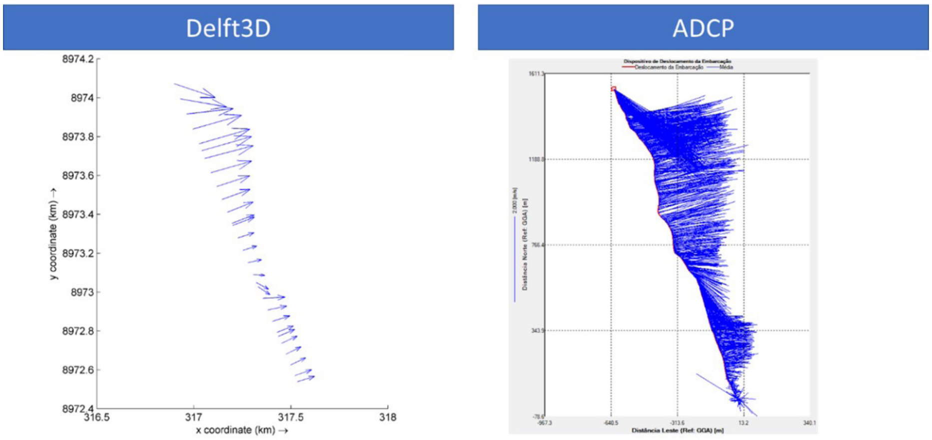

Figure 12. Direction and intensity of horizontal velocities (vertical averages) along the ADCP section - High flow - 25th Feb 2019.

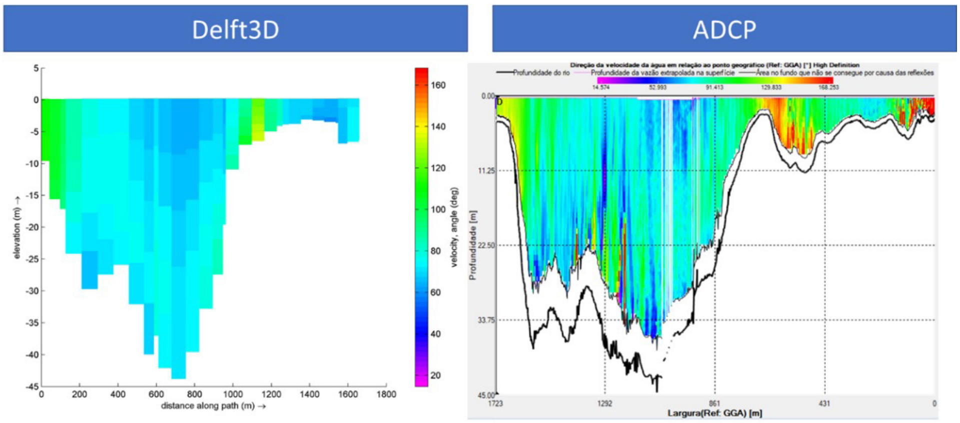

Figure 13. Angle of horizontal velocities - High flow - 25th Feb 2019.

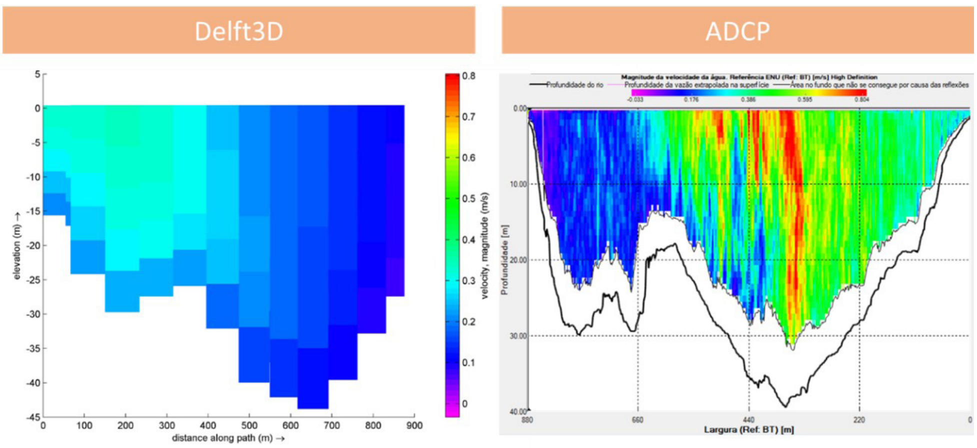

Figure 14. Transect illustrating magnitude of horizontal velocities - 16th Aug 2018.

Conventional water level comparison has been done to adjust the Manning coefficient, resulting in water level differences between measurements and simulations of less then 10 cm. Manning's coefficient was adjusted to ensure that the water level along the reservoir was consistent with the water level in the HEC-RAS model (Energia Sustentável do Brasil, 2020), which was previously configured for various scenarios, and also with the water level record at the Bananal limnimetric ruler.

Hydrodynamic characterization

Cross-sectional and longitudinal sections of the reservoir (Figure 9) were drawn to represent the water velocity results.

Figure 15 shows the magnitudes and directions of the horizontal surface velocities along the Jirau HPP reservoir for each of the scenarios. Figure 16 shows these velocities in longitudinal section from upstream to downstream. Figure 17 and Figure 18 show the magnitude of velocities in cross sections on the right bank (RB) and left bank (LB), respectively, for each scenario, and Figure 19 shows the magnitude of the velocities in the cross section through the retention structures, called S11.

Comparing the images in Figure 17, it can be seen that the maximum velocities shift to the right of the RBPH and the velocities in the spillway decrease with the introduction of the log boom. This effect was also observed in S11 (Figure 19), where there is a shift of the velocities to the left and right relative to the respective log boom lines.

On the left bank (Figure 18), the flow remained the same, so the velocities were also similar between both scenarios, regardless of the log boom.

It was possible to observe the effect of the log booms on the flow: in the cells where the log booms are positioned (surface), there is no passage of water, so the velocity is zero and is represented by a red circle in Figure 16 and Figure 19. However, a current is formed parallel to the right log boom line (Figure 20).

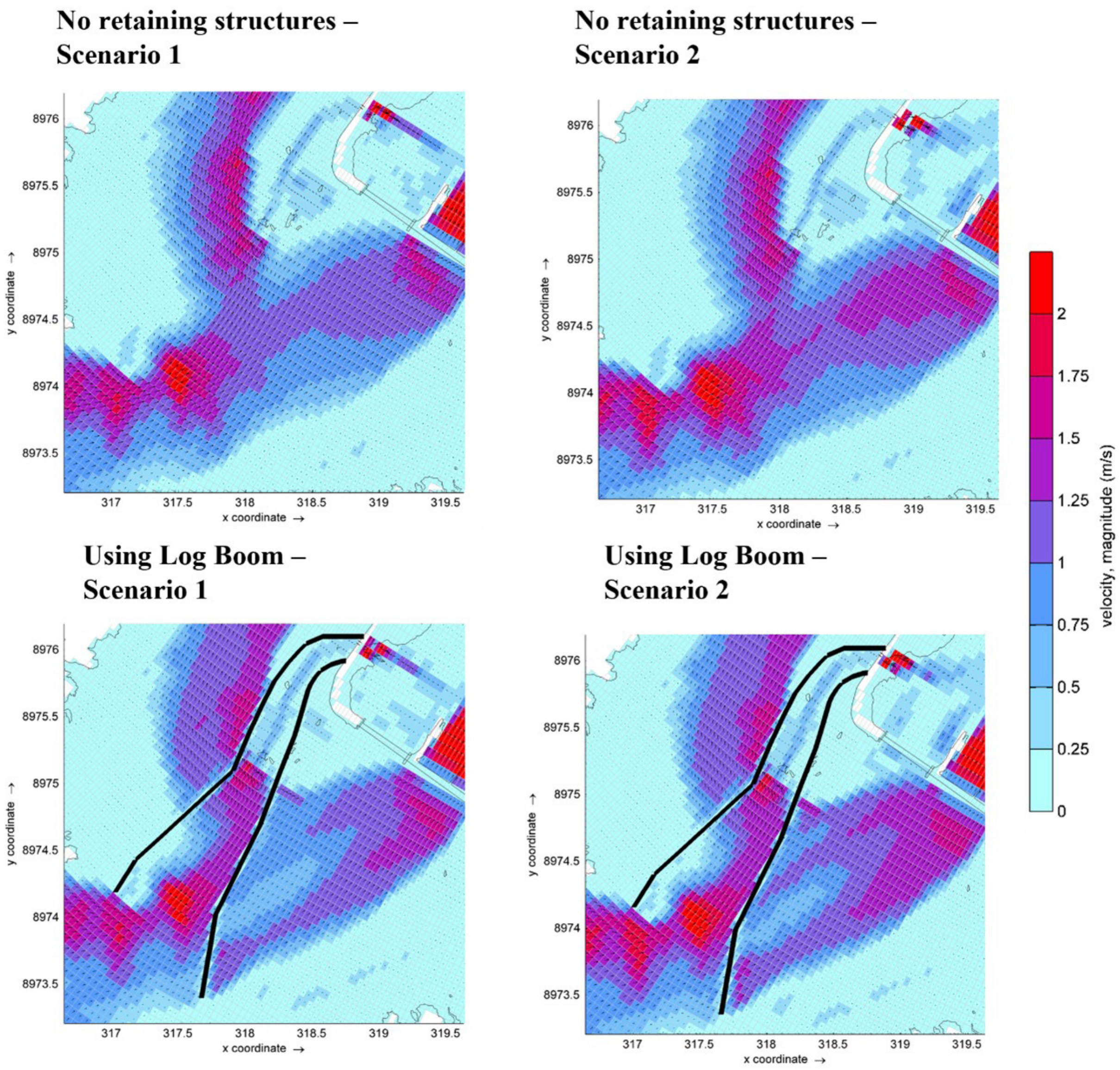

Figure 15. Magnitude of horizontal surface velocities along the Jirau HPP reservoir.

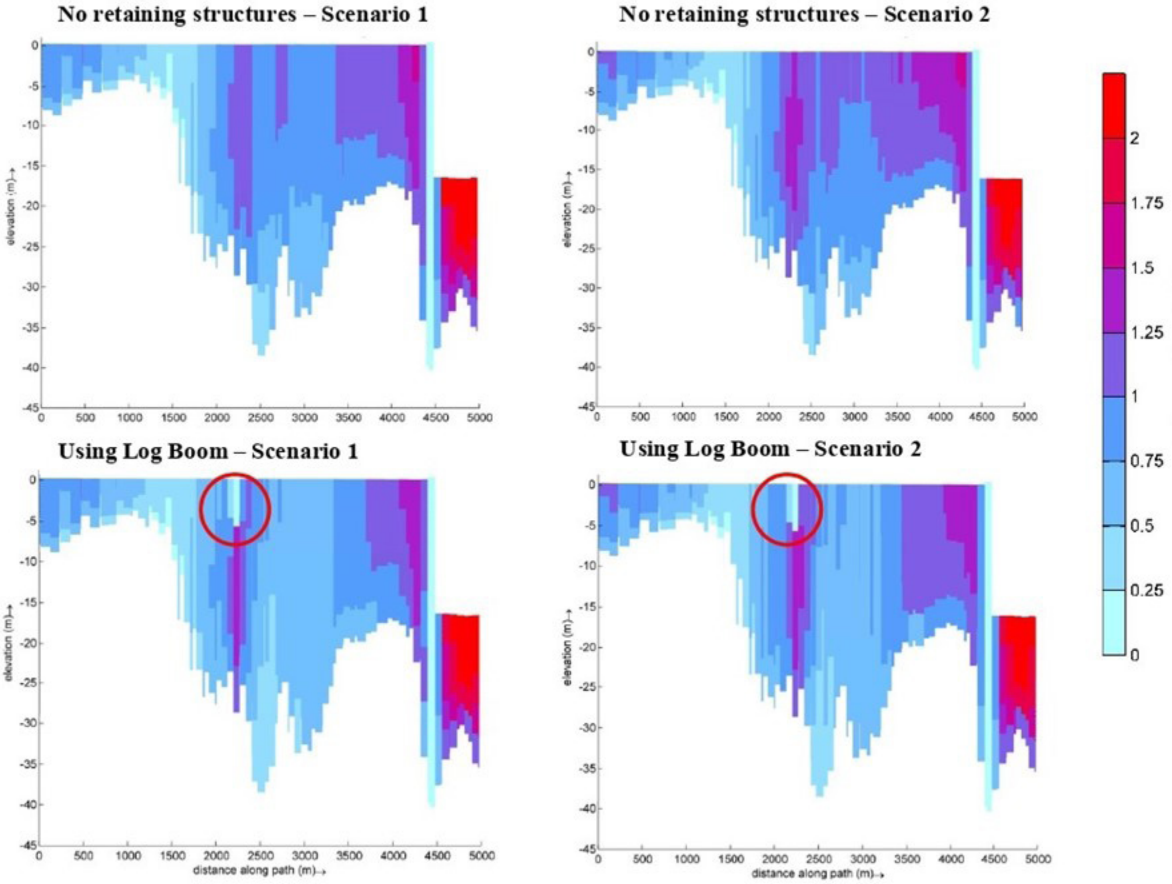

Figure 16. Magnitude of horizontal velocities in the longitudinal section along the Jirau HPP reservoir.

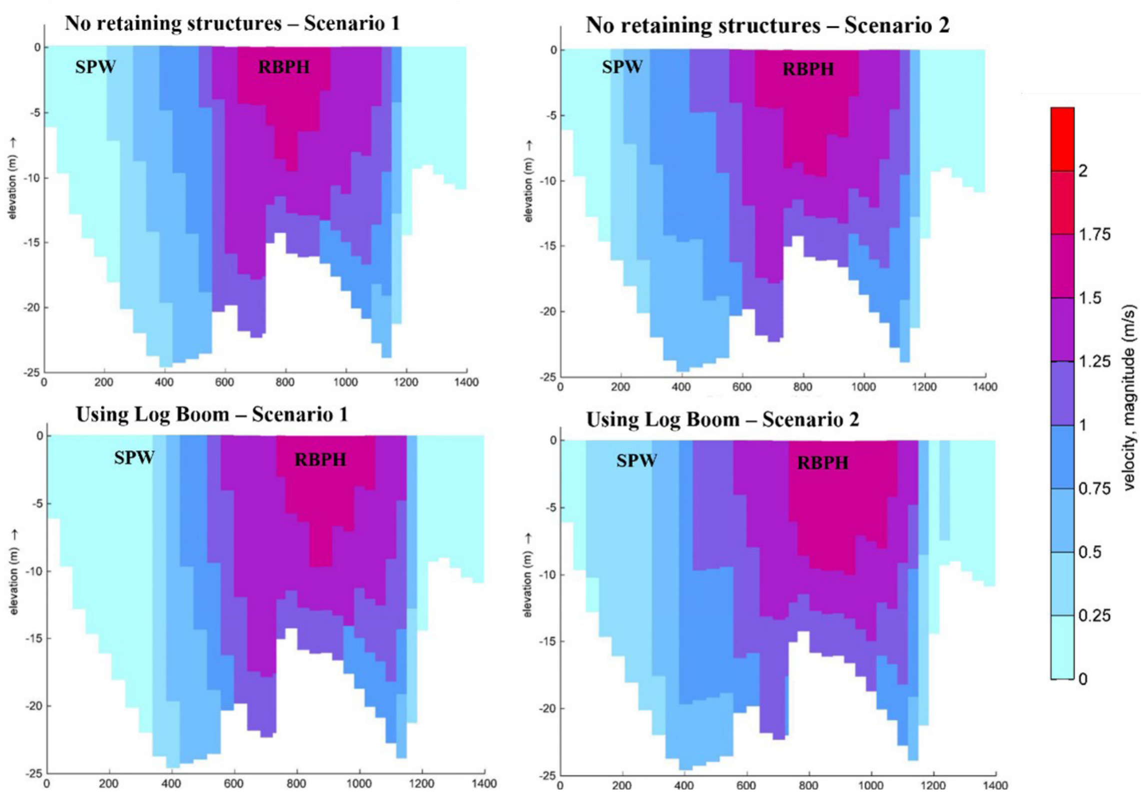

Figure 17. Magnitude of velocities on the right bank of the Jirau HPP reservoir for each scenario.

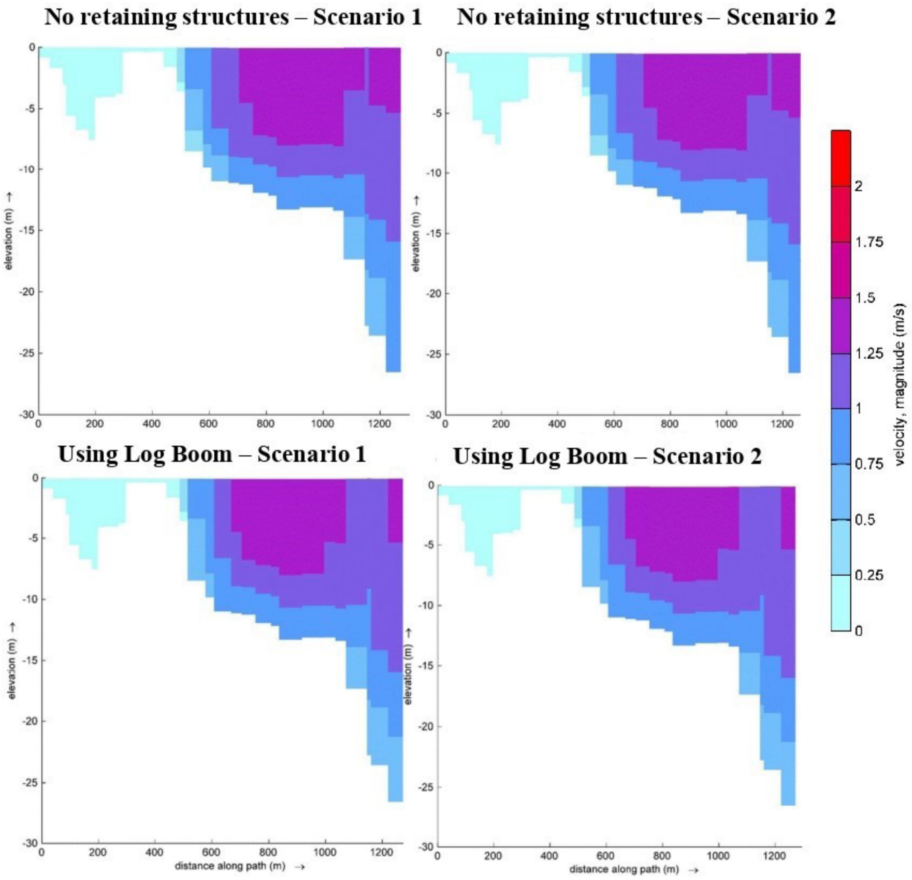

Figure 18. Magnitude of velocities at transect on the left bank of the Jirau HPP reservoir for each scenario.

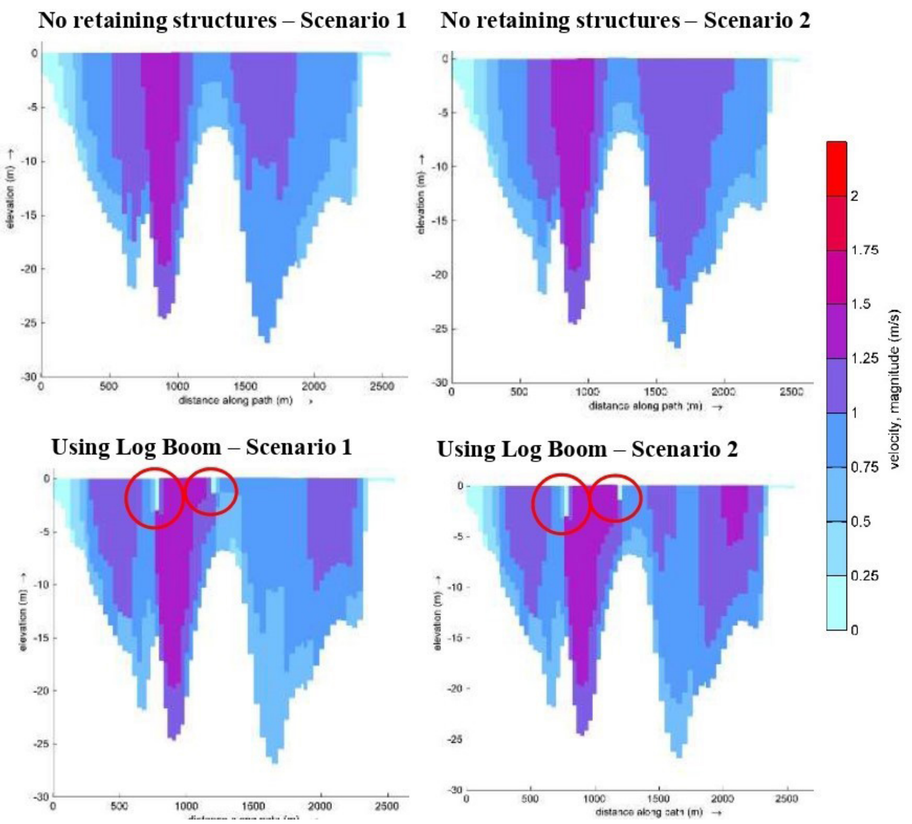

Figure 19. Magnitude of velocities in the section named S11 through the log boom.

Particle tracking results

The three-dimensional behavior of the particle trajectories for each scenario was analyzed. Figure 21 shows the trajectory of the particles, where the color represents the depth of the particle, and the black lines represent the log boom. Particles released at the surface remained in shallower regions (less than 10 meters) until they reached the bottleneck region, where the depths tended to be greater. After passing through this region, the particle depths decrease again due to the changing bathymetry. Figure 22 shows the trajectories for each scenario, with the color representing the destination of the particle. It is emphasized that even with the spillway closed, it is still possible to observe particles reaching this destination. This occurs due to the hydrodynamics of the area.

The particle distribution was consistent with the flow distribution for both situations, with small variations in the percentages. These variations indicated that the log boom insertion reduced the incidence of particles in the left bank powerhouse, however only in scenario 2 the incidence of particles in the right bank powerhouse was reduced while in the scenario 1 increased by 4%. The percentage of particles going into the spillway increased with the insertion of log boom. And the log-spillway was not attractive because it has a lower flow rate than the other structures. Figure 23 shows the statistical results.

Figure 24 shows the histogram of particle depths. After calibration of the particle model and testing for simulation, this distribution was close to the field log monitoring data, thus containing most of the logs on the surface. The presence of log boom slightly reduces the percentage of particles on the surface.

Figure 25 to Figure 28 show the influence of the log boom on the vertical distribution of particles for the two operating scenarios. It is possible to observe the particles deflecting from the retaining structure, passing underneath. For this reason, the percentage of particles on the surface decreases when log boom is present.

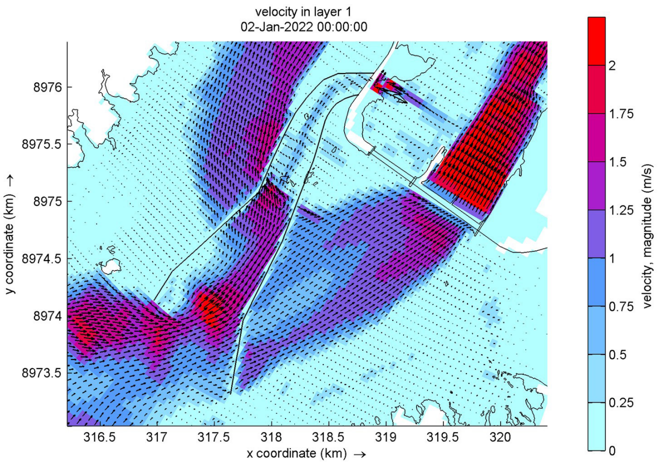

Figure 20. Velocities near the log boom for Scenario 1.

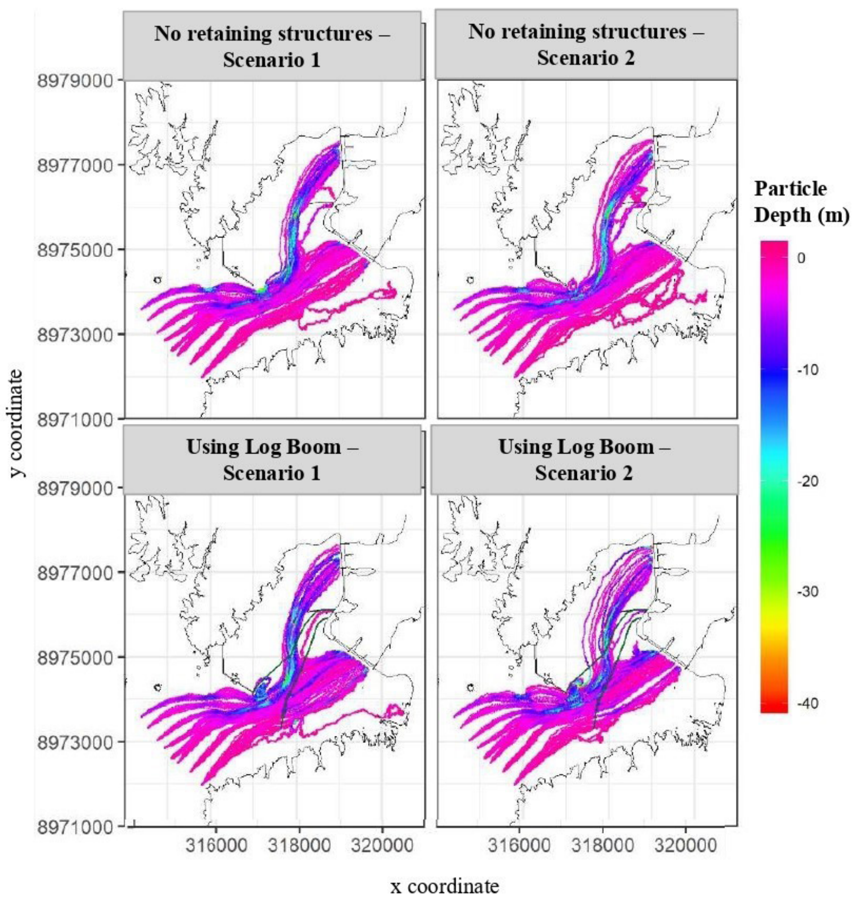

Figure 21. Particle trajectory and depth for each scenario in the UHE Jirau reservoir.

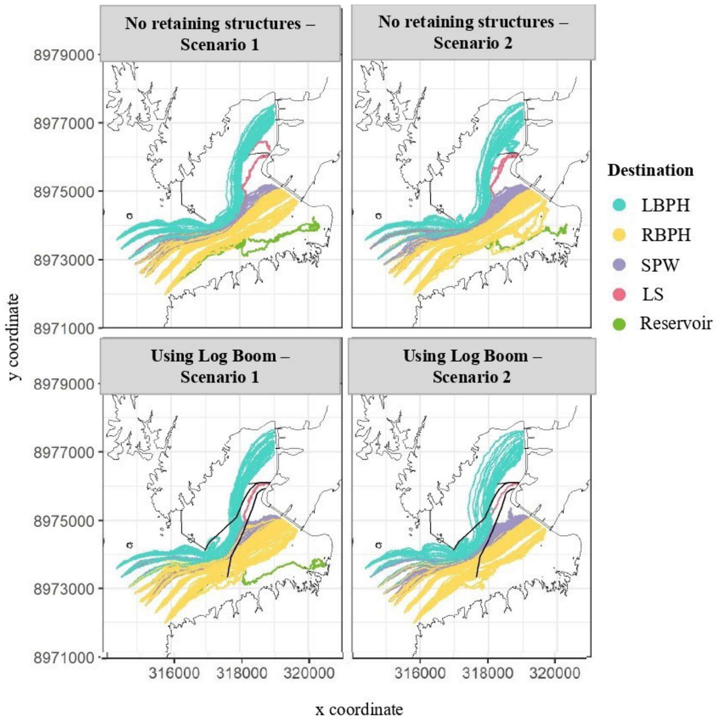

Figure 22. Particle trajectory and destination for each scenario in the UHE Jirau reservoir.

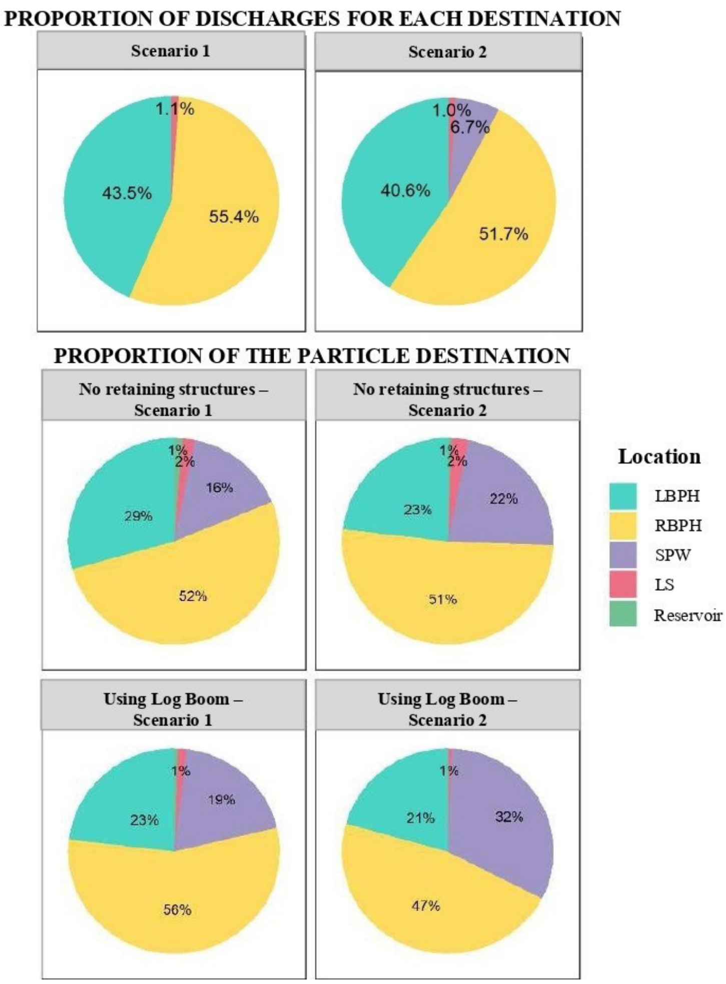

Figure 23. Statistical comparison between the proportion of discharges and the proportion of particle destination.

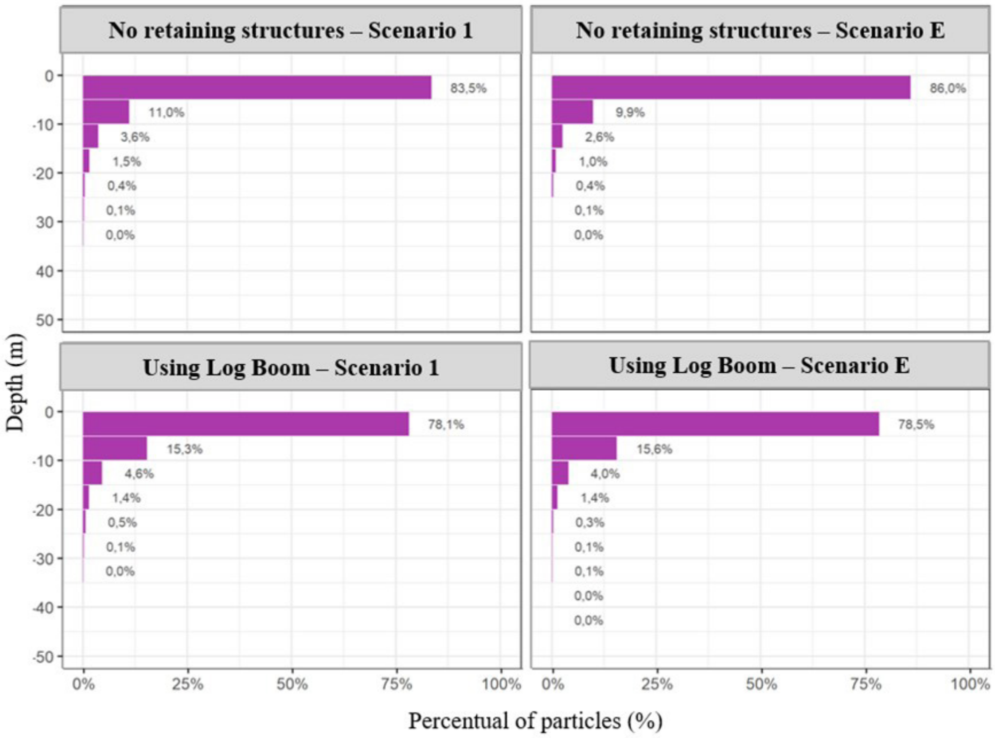

Figure 24. Vertical particle distribution histogram.

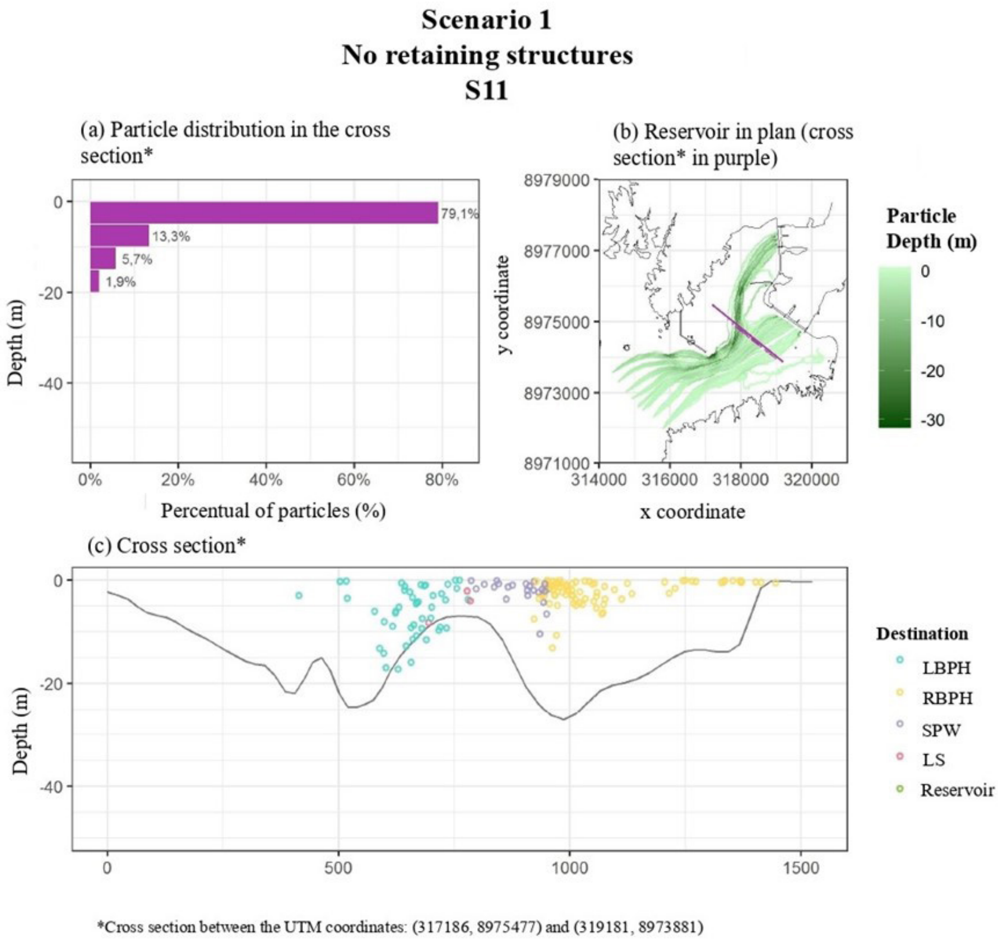

Figure 25. Vertical particle distribution in S11 for scenario 1 - no retention structures.

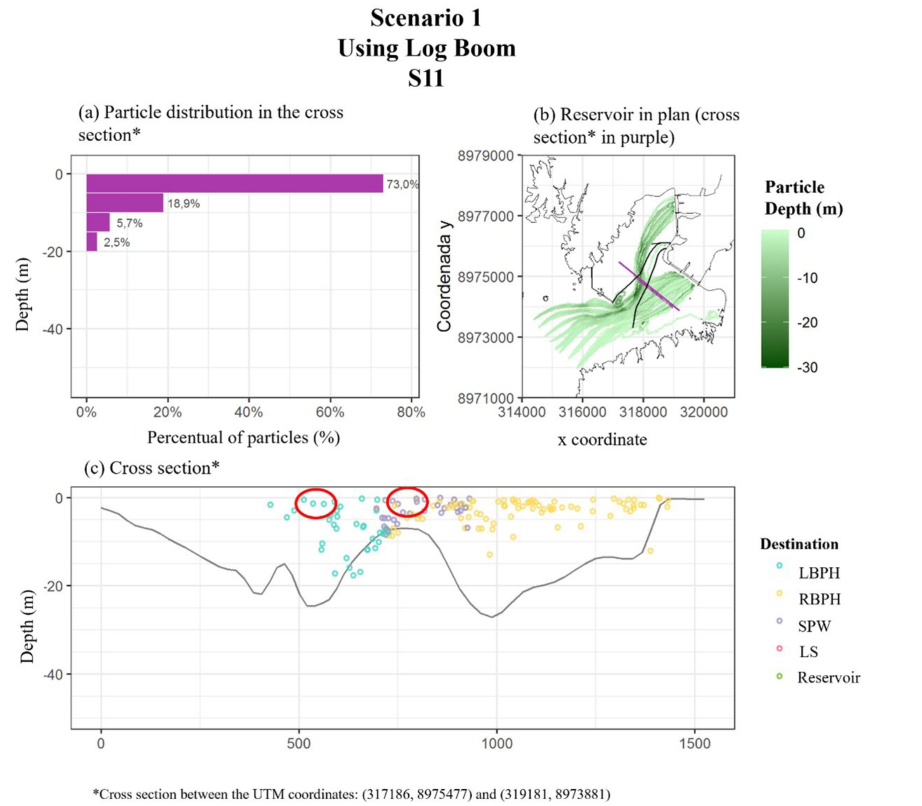

Figure 26. Vertical particle distribution in S11 for scenario 1 - using log booms.

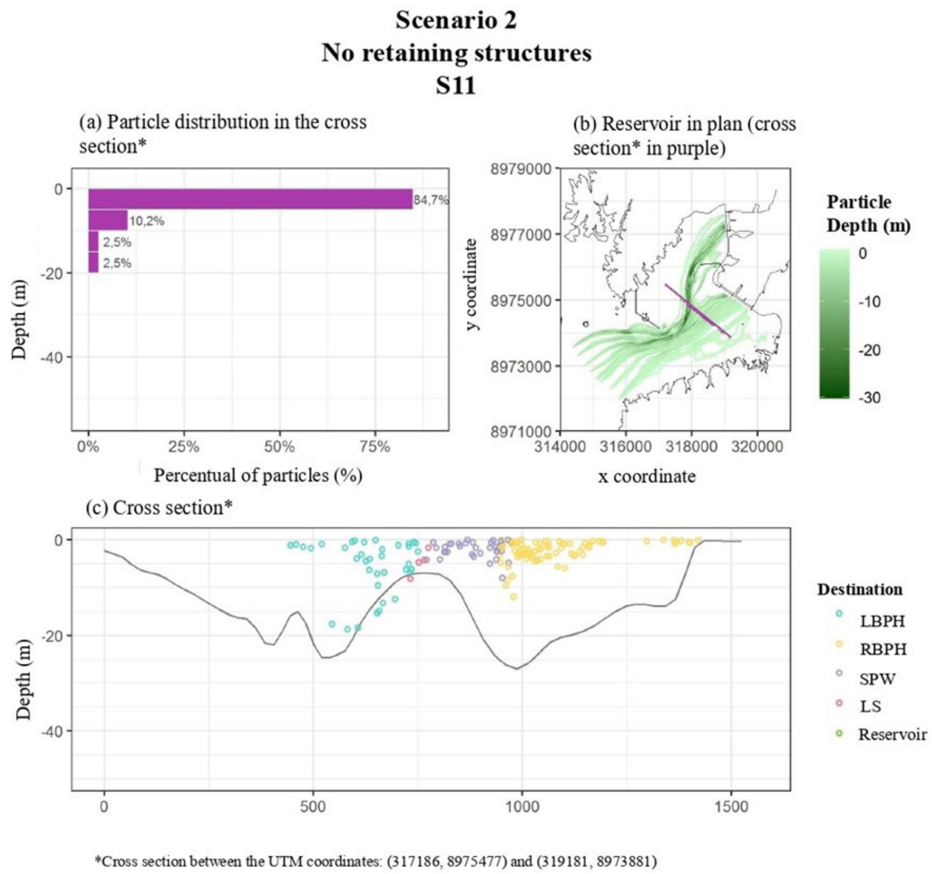

Figure 27. Vertical particle distribution in S11 for scenario 2 - no retention structures.

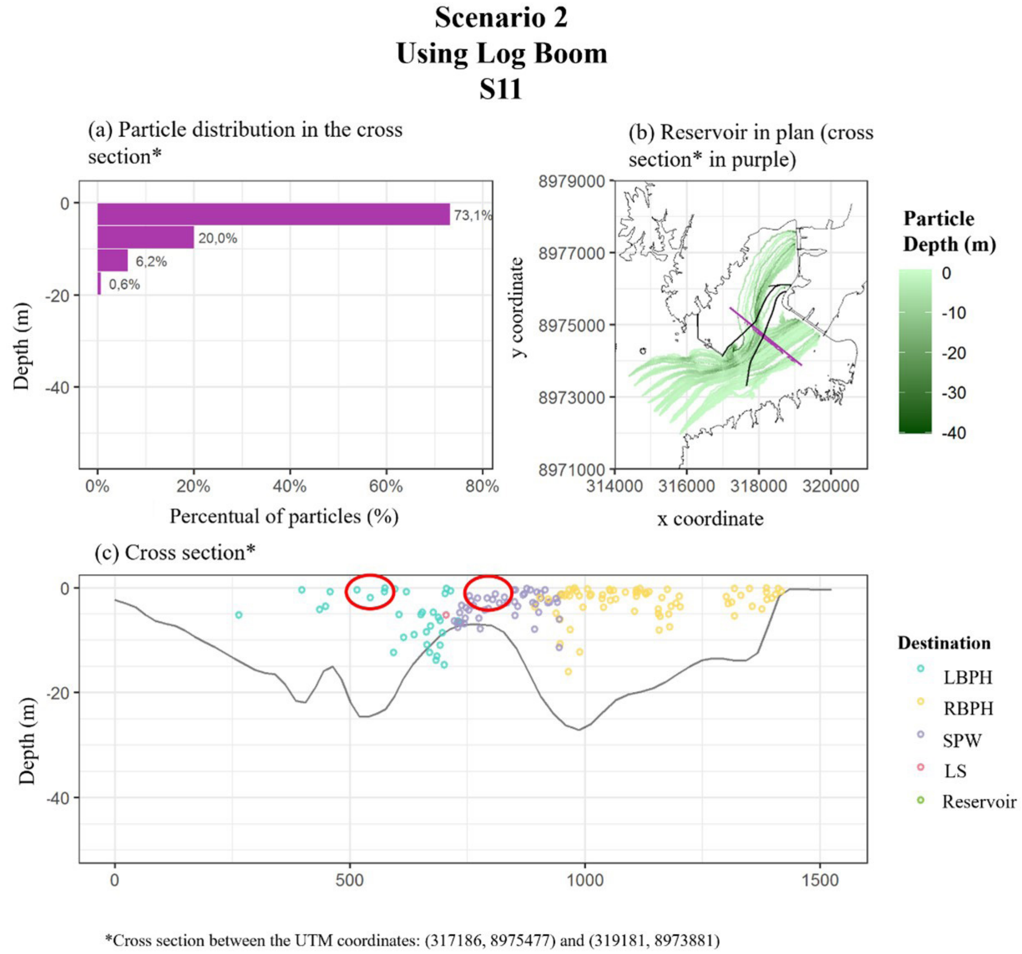

Figure 28. Vertical particle distribution in S11 for scenario 2 - using log booms.

CONCLUSIONS

The results presented for calibration showed that there are some deficiencies, and it has been concluded that the model is able to reproduce the general hydrodynamics of the region of interest, especially for higher flows, but shows limitations in the representation of regions with complex hydrodynamics such as the convergence region (ADCP section) and vertical profiles with strong secondary currents.

With the hydrodynamic modeling, it was possible to better understand the water dynamics in different scenarios, including hydraulic variables, retaining structures and reservoir operation, and it was possible to represent log transport, which will subsidize Jirau HPP in its operation and improvement projects in the log booms, for example.

The particle trajectories were consistent with the flow distribution and the insertion of the log booms.

The right powerhouse region was easily reached after passing through the bottleneck, even considering the log boom effect. The log-spillway structure was not effective to discharge the woody material, taking into account the modeled operating rules, since the main current flow was directed toward the higher flow structures, and only a small percentage (1% to 2%) reached the log-spillway.

The particles have no mass or forces acting on them, they just follow the flow with diffusive components, so when they find some retaining structure, they tend to deflect by passing underneath.

It was possible to represent the logs through particles in the three-dimensional model, this simulation does not allow assigning shapes, volume or mass to the particles. Therefore, there was no significant influence of the retaining structures on the retention of this woody material, if represented in this way, which differs from reality.

In general, the particles follow the mean flow field with an additional arbitrary movement corresponding to turbulent intensities. The structures affect the mean flow field, thus change the particle tracks and turbulent characteristics close to them. However, particles do not get stuck at structures, as wood would do. Consequently, wood accumulation is not accurately predicted with this approach, but the model can be used to analyze different operational features to improve log transport.

With respect to the context of hydroelectric reservoirs, the literature search has shown that studies in this area are still lacking. There are few cases that have been validated in fields and the parameters for modeling have not yet been fully clarified. Some models have been applied to simplified rectangular channel situations, but they are not applicable to the size and complexity of Jirau and its number of wood material.

ACKNOWLEDGEMENTS

Project regulated by the National Agency of Electric Energy (Agência Nacional de Energia Elétrica – ANEEL) and developed within the scope of Jirau Energia's R&D program, entitled "Desenvolvimento de metodologia integrada para o monitoramento do transporte de material lenhoso para a concepção de sistema de manejo de troncos submersos - DMIMMAD (06631-0014/2020)". Tobias Bleninger acknowledges the productivity stipend from the National Council for Scientific and Technological Development – CNPq, grant no. 312211/2020-1, call no. 09/2.

REFERENCES

Bladé, E., Sánchez-Juny, M., & Ruiz-Villanueva, V. (2016). Strategies in the 2D numerical modelling of wood transport in rivers. In *Proceedings of the Eight International Conference on Fluvial Hydraulics*, St. Louis, MO, USA.

Construserv Serviços Gerais Ltda. (2020). *Plano de trabalho para a campanha de batimetria do reservatório da UHE Jirau – Rio Madeira.* Maringá: Construserv Serviços Gerais Ltda.

Deltares. (2023a). *Delft3D-FLOW, Simulation of multi-dimensional hydrodynamic flows and transport phenomena, including sediments, User Manual Hydro-Morphodynamics.* Retrieved in 2023, August 25, from https://oss.deltares.nl/web/delft3d/manuals

Deltares. (2023b). *D-Waq part, simulation of mid-field water quality and oil spills, using, particle tracking, user manual D-water quality.* Retrieved in 2023, August 25, from https://oss.deltares.nl/web/delft3d/manuals

Energia Sustentável do Brasil – ESBR. (2009). *Nota técnica - Anexo 1 - Revisão do Estudo de Vazão máxima de dimensionamento de vertedouro para a UHE Jirau.* Porto Velho: ESBR. 110-JI-CEP-0024-09.

Energia Sustentável do Brasil – ESBR. (2019). *PSB – Plano de Segurança de Barragem UHE Jirau.* Porto Velho: ESBR. PL-CIVI-US-001.

Energia Sustentável do Brasil – ESBR. (2020). *Estudo de remanso 2020: atualização do modelo hidráulico do reservatório*. Porto Velho: ESBR. RT-CHID-RS-001-20.

Lactec. (2021). *Desenvolvimento de metodologia integrada para o monitoramento do transporte de material lenhoso para a concepção de sistema de manejo de troncos submersos – DMIMMAD. Relatório técnico – etapa 3: revisão bibliográfica.* Curitiba: Lactec.

Lactec. (2023). *Desenvolvimento de metodologia integrada para o monitoramento do transporte de material lenhoso para a concepção de sistema de manejo de troncos submersos – DMIMMAD. Relatório final – etapa 6: caracterização física dos troncos.* Curitiba: Lactec.

Ruiz Villanueva, V., Bladé Castellet, E., Díez-Herrero, A., Bodoque, J. M., & Sánchez-Juny, M. (2013). Two-dimensional modelling of large wood transport during flash floods. *Earth Surface Processes and Landforms*, *39*(4), 438-449. http://dx.doi.org/10.1002/esp.3456.

Ruiz-Villanueva, V., Bladé, E., Sánchez-Juny, M., Marti-Cardona, B., Díez-Herrero, A., & Bodoque, J. M. (2014). Two-dimensional numerical modeling of wood transport. *Journal of Hydroinformatics*, *16*(5), 1077-1096. http://dx.doi.org/10.2166/hydro.2014.026.

Ruiz-Villanueva, V., Piégay, H., Gurnell, A. M., Marston, R. A., & Stoffel, M. (2016). Recent advances quantifying the large wood dynamics in river basins: new methods and remaining challenges. *Reviews of Geophysics*, *54*(3), 611-652. http://dx.doi.org/10.1002/2015RG000514.

Schalko, I. (2018). *Modeling hazards related to large wood in rivers* (Doctoral thesis). ETH Zurich, Austria. https://doi.org/10.3929/ethz-b-000293084.

Schalko, I., Schmocker, L., Weitbrecht, V., & Boes, R. (2019). Laboratory study on wood accumulation probability at bridge piers. *Journal of Hydraulic Research*, *58*(4), 566-581.

Seo, J. I., Nakamura, F., & Chun, K. W. (2010). Dynamics of large wood at the watershed scale: a perspective on current research limits and future directions. *Landscape and Ecological Engineering*, *6*, 271-287. http://dx.doi.org/10.1007/s11355-010-0106-3.

Zuanon, J., & Vilara, G. T. (2005). Associação entre peixes e raízes adventícias de plantas epífitas em afluentes do alto rio Madeira. In *VII Congresso de Ecologia do Brasil*, Caxambu, MG.

Authors contributions

Isabela Rodrigues Caldatto: Data processing, analysis and discussion of results and manuscript writing.

Ana Carolina Canossa Becker: Data processing, analysis and discussion of results and manuscript writing.

Tobias Bleninger: Discussion of results and manuscript review.

Bruna Arcie Polli: Discussion of results and manuscript review.

Rubem Luiz Daru: Data processing, discussion of results and manuscript writing.

Renato Penteado: Discussion of results and manuscript writing.

Claudiney Freitas: Manuscript review.

Editor-in-Chief: Adilson Pinheiro

Associated Editor: Iran Eduardo Lima Neto

APPENDIX A. CALIBRATION SCENARIOS.

Figures A1 to A12 present the remaining calibration scenarios for intermediate, low, and lower flow rates.

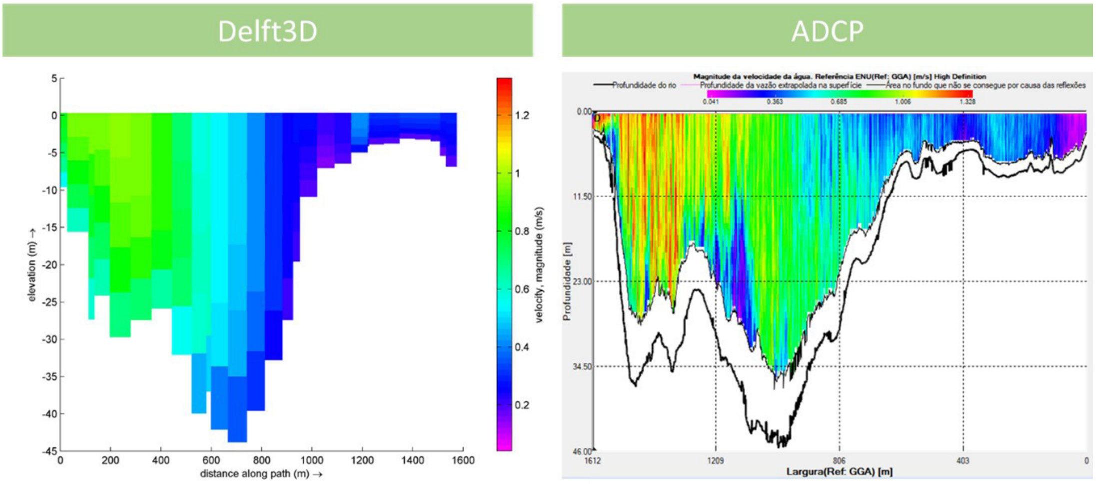

Figure A1. Transect illustrating magnitude of horizontal velocities - Intermediate flow: 20,072 m^3/s - 11th Feb 2017.

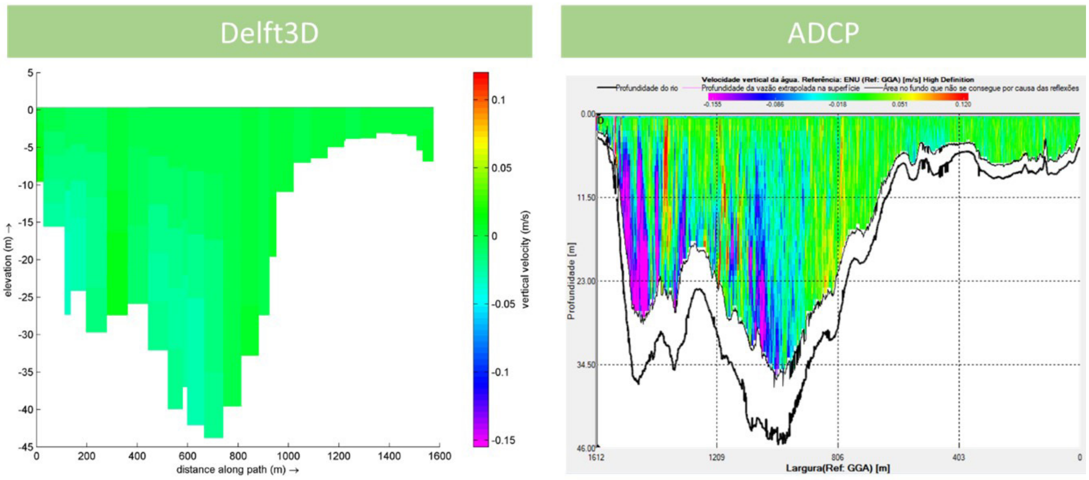

Figure A2. Transect illustrating magnitude of vertical velocities - Intermediate flow: 20,072 m^3/s - 11th Feb 2017.

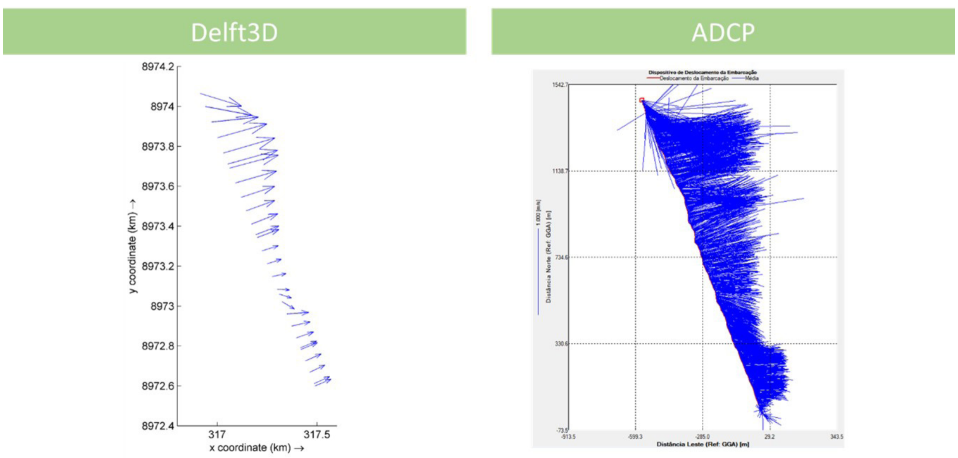

Figure A3. Direction and intensity of horizontal velocities (vertical averages) along the section - Intermediate flow: 20,072 m^3/s - 11th Feb 2017.

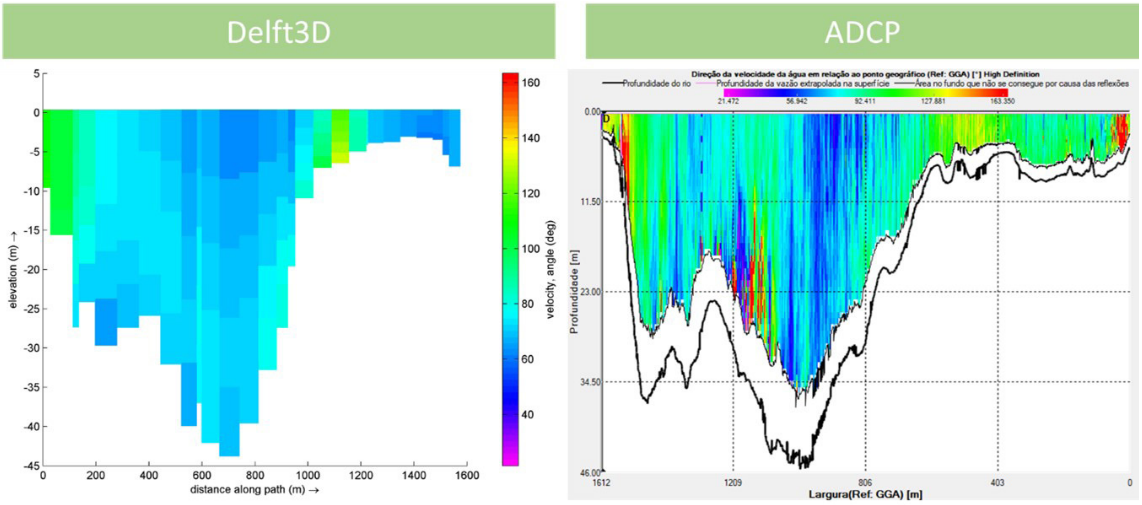

Figure A4. Angle of horizontal velocities - Intermediate flow: 20,072 m^3/s - 11th Feb 2017.

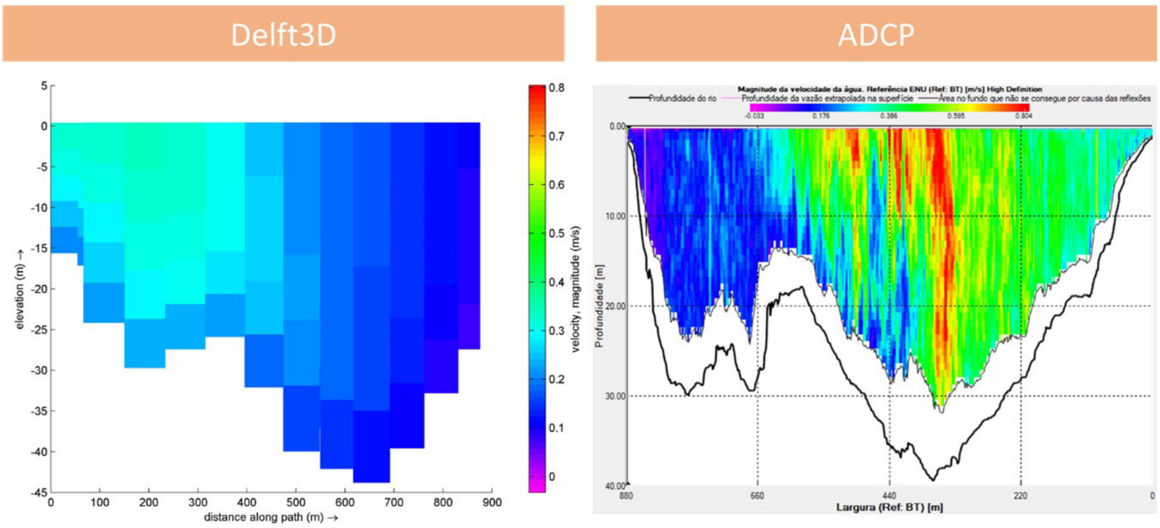

Figure A5. Transect illustrating magnitude of horizontal velocities - Low flow: 6,808 m^3/s – 16th Aug 2018.

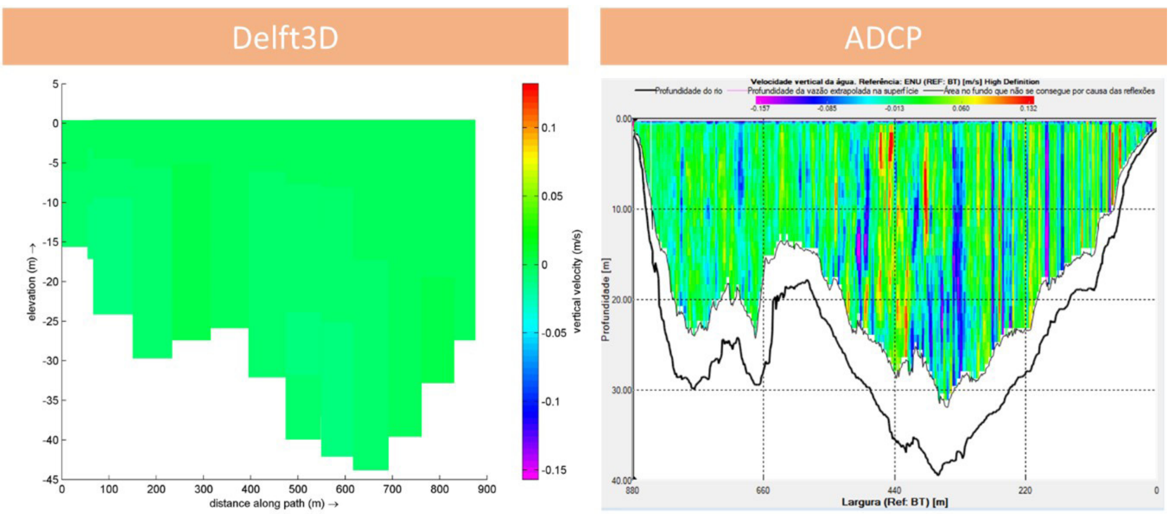

Figure A6. Transect illustrating magnitude of vertical velocities - Low flow: 6,808 m^3/s – 16th Aug 2018.

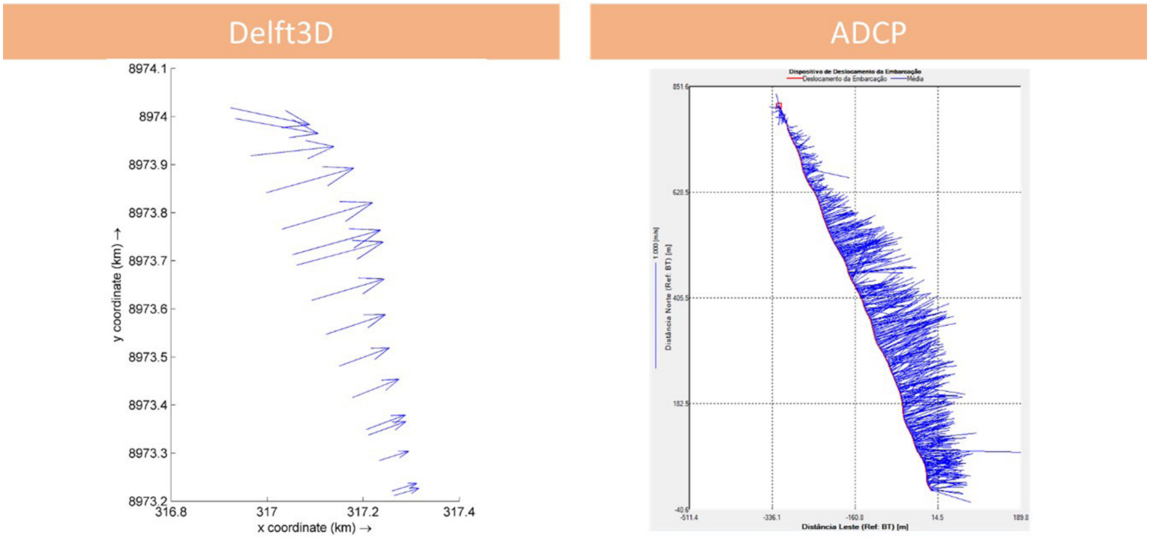

Figure A7. Direction and intensity of horizontal velocities (vertical averages) along the section - Low flow: 6,808 m^3/s – 16th Aug 2018.

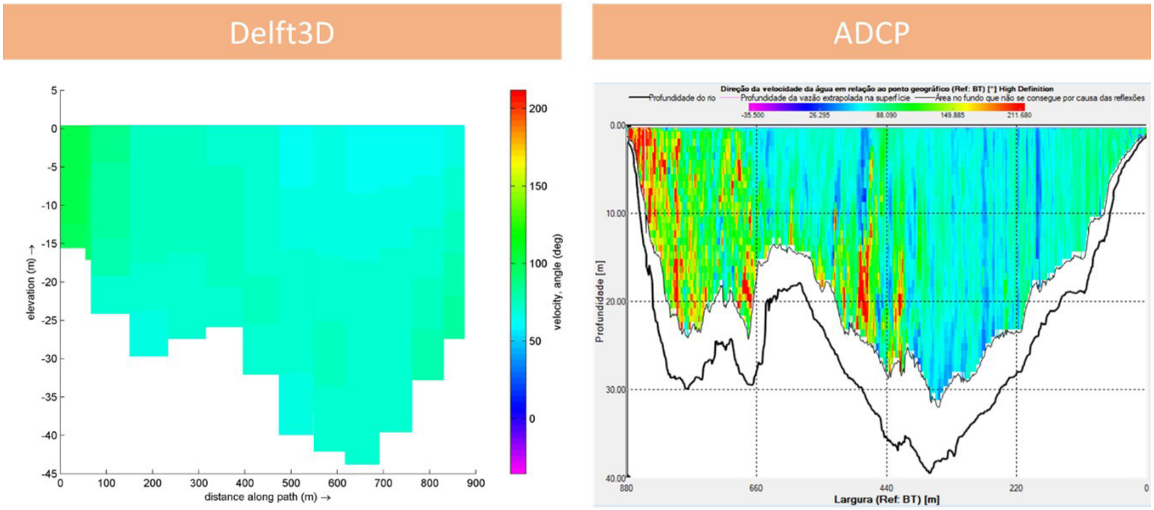

Figure A8. Angle of horizontal velocities - Low flow: 6,808 m^3/s – 16th Aug 2018.

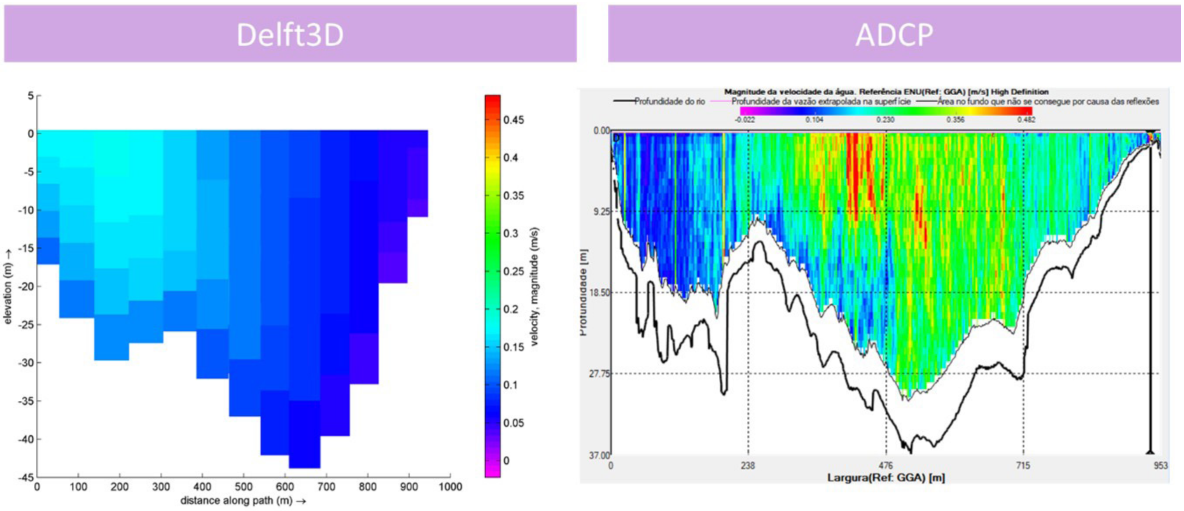

Figure A9. Transect illustrating magnitude of horizontal velocities - Lower flow: 3,599 m^3/s – 09th Aug 2016.

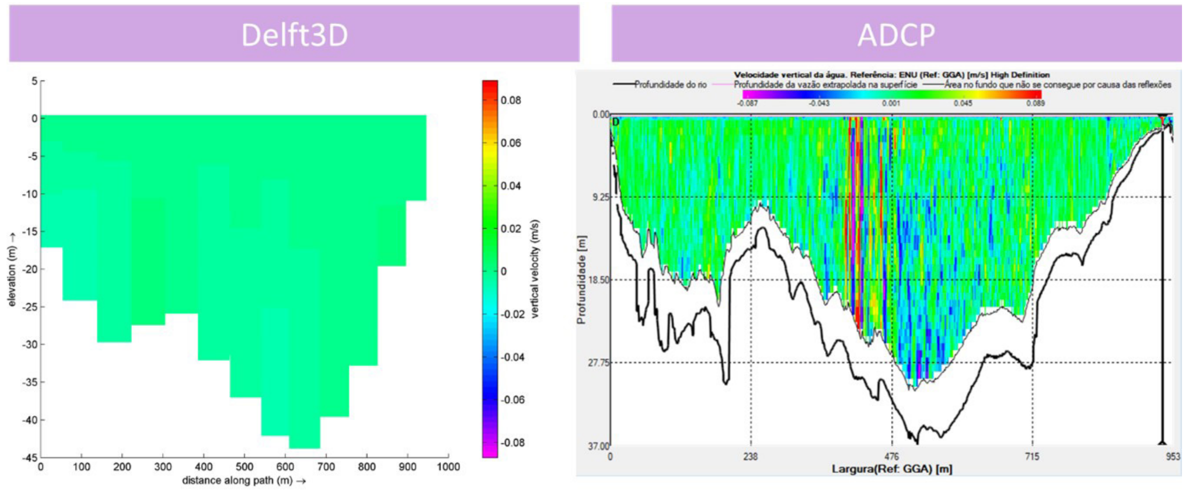

Figure A10. Transect illustrating magnitude of vertical velocities - Lower flow: 3,599 m^3/s – 09th Aug 2016.

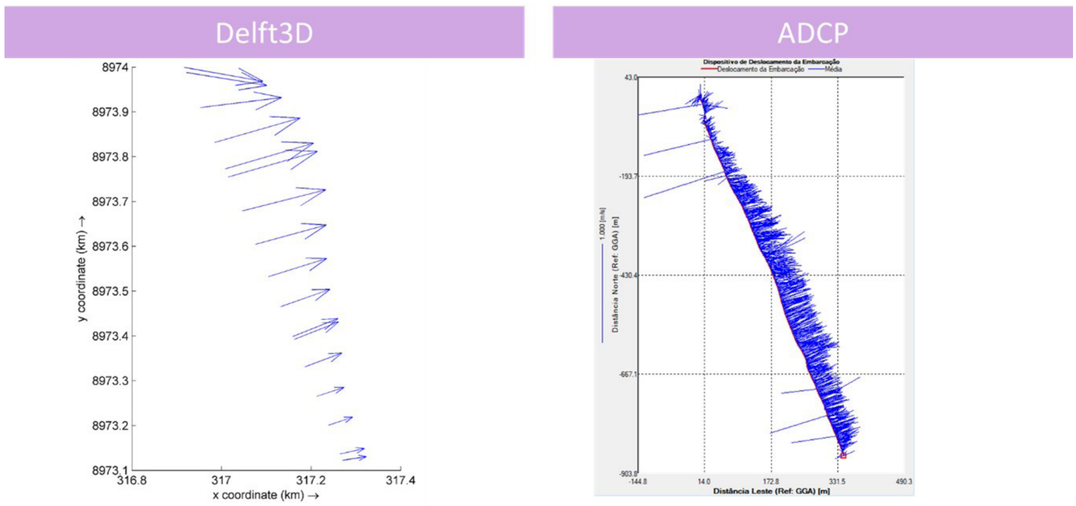

Figure A11. Direction and intensity of horizontal velocities (vertical averages) along the section - Lower flow: 3,599 m^3/s – 09th Aug 2016.

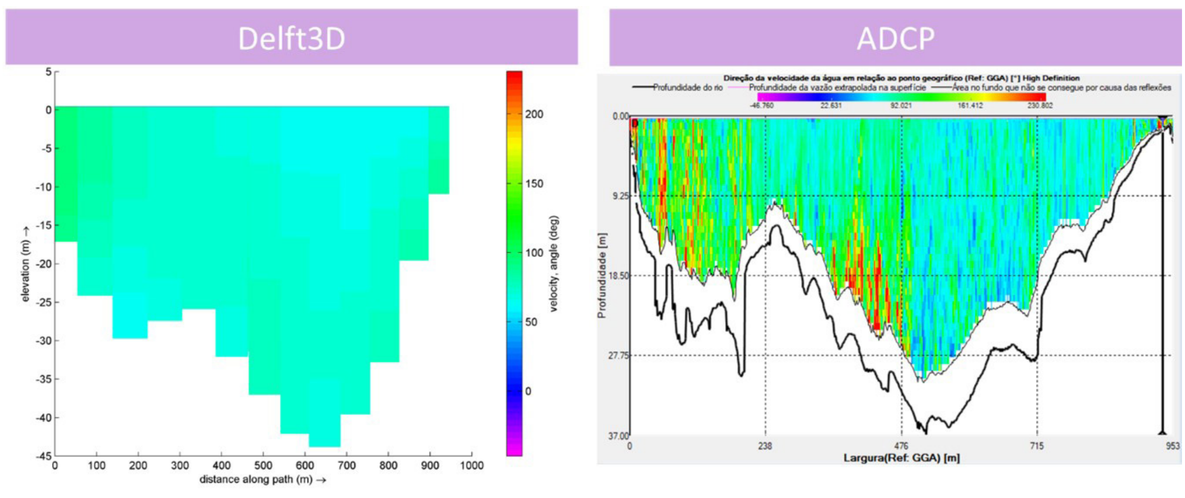

Figure A12. Angle of horizontal velocities - Lower flow: 3,599 m^3/s – 09th Aug 2016.